Atmospheric
Chemistry
and Physics
Discussions

1   Contributions of Trans-boundary Transport to the Summertime Air Quality in Beijing, China

2

3   Jiarui Wu[1], Guohui Li[1*], Junji Cao[1*], Naifang Bei[2], Yichen Wang[1], Tian Feng[1, 2], Rujin Huang[1], Suixin Liu[1],

4   Qiang Zhang[3], and Xuexi Tie[1]

5

6   [1]Key Lab of Aerosol Chemistry and Physics, SKLLQG, Institute of Earth Environment, Chinese Academy of

7   Sciences, Xi'an, China

8   [2]School of Human Settlements and Civil Engineering, Xi'an Jiaotong University, Xi'an, Shaanxi, China

9   [3] Department of Environmental Sciences and Engineering, Tsinghua University, Beijing, China

10   [*]Correspondence to: Guohui Li (ligh@ieecas.cn) and Junji Cao (jjcao@ieecas.cn)

11

12   **Abstract**: In the present study, the WRF-CHEM model is used to evaluate the contributions

13   of trans-boundary transport to the air quality in Beijing during a persistent air pollution

14   episode from 5 to 14 July 2015 in Beijing-Tianjin-Hebei (BTH), China. Generally, the

15   predicted temporal variations and spatial distributions of $PM_{2.5}$ (fine particulate matter), O_3

16   (ozone), and NO_2 are in good agreement with observations in BTH. The WRF-CHEM model

17   also reproduces reasonably well the temporal variations of aerosol species compared to

18   measurements in Beijing. The factor separation approach is employed to evaluate the

19   contributions of trans-boundary transport of emissions outside of Beijing to the $PM_{2.5}$ and O_3

20   levels in Beijing. On average, in the afternoon during the simulation episode, the pure local

21   emissions contribute 22.4% to the O_3 level in Beijing, less than 36.6% from pure emissions

22   outside of Beijing. The O_3 concentrations in Beijing are decreased by 5.1% in the afternoon

23   due to interactions of local emissions with those outside of Beijing. The pure emissions

24   outside of Beijing play a dominant role in the $PM_{2.5}$ level in Beijing, with a contribution of

25   61.5%, much more than 13.7% from pure Beijing local emissions. The emissions interactions

26   enhance the $PM_{2.5}$ concentrations in Beijing, with a contribution of 5.9%. Therefore, the air

27   quality in Beijing is primarily determined by the trans-boundary transport of emissions

28   outside of Beijing during summertime, showing that the cooperation with neighboring

29   provinces to mitigate pollutant emissions is a key for Beijing to improve air quality.

30   Considering the uncertainties in the emission inventory and the meteorological field

31   simulations, further studies need to be performed to improve the WRF-CHEM model

32   simulations to reasonably evaluate trans-boundary transport contributions to the air quality in

33   Beijing for supporting the design and implementation of emission control strategies.

Atmospheric
Chemistry
and Physics
Discussions

1 Introduction

34

35   Beijing, the capital of China, has become an environmentally stressed city due to

36   growing population, increasing transportation activity, and city expansion (Parrish and Zhu,

37   2009). Beijing is situated in northeastern China, surrounded from the southwest to the

38   northeast by the Taihang Mountains and the Yanshan Mountains and open to the North China

39   Plain (NCP) in the south and east. Unfortunately, NCP has become one of the most polluted

40   areas in China due to rapid industrialization and urbanization (Zhang et al., 2013). When

41   south or east winds are prevalent in NCP, air pollutants originated from NCP are transported

42   to Beijing and surrounding areas and subject to be accumulated due to the mountain blocking,

43   causing heavy air pollution in Beijing (Long et al., 2016).

44   PM$_{2.5}$ (fine particulate matter) and O$_3$ (ozone) are considered to be the most serious air

45   pollutants of concern in Beijing during summertime (e.g., Xie et al., 2015; Zheng et al., 2015;

46   Chen et al., 2015; Wang et al., 2016). The mean summertime PM$_{2.5}$ mass concentration is

47   about 80 μg m^{-3} in 2013 (Li et al., 2015a), exceeding the second grade of National Ambient

48   Air Quality Standards (NAAQS) in China and also higher than the average PM$_{2.5}$

49   concentration of 78.1μg m^{-3} during the period from 2004 to 2012 (Liu et al., 2015). During

50   haze pollution events in summer 2014, the PM$_{2.5}$ concentration generally reaches 100 μg m^{-3},

51   and even exceeds 150 μg m^{-3} in Beijing (Wang et al., 2016). An increasing O$_3$ trend has been

52   observed in Beijing from 2002 to 2010 (Wang et al., 2012; Wang et al., 2013). The average

53   maximum 1-h O$_3$ concentration has been reported to achieve 140 μg m^{-3} during summertime

54   of 2013 in Beijing (Wang et al., 2014a). Wang et al. (2016) have demonstrated that the

55   summertime O$_3$ mass concentration holds a high level in 2014 in Beijing, with a daily

56   average of up to 110 µg m^{-3}. Chen et al. (2015) have further shown that the average

57   maximum daily O$_3$ concentrations are higher than 150 µg m^{-3} during the summer in 2015 at

58   most of monitoring sites in Beijing.

59   In recent years, Beijing has implemented aggressive emission control strategies to

60   ameliorate the air quality (Parrish and Zhu, 2009). Both NO$_x$ (NO+NO$_2$) and total VOCs

61   (volatile organic compounds) in Beijing have decreased linearly since 2002, while the

62   daytime average O$_3$ concentration still increases rapidly (Tang et al., 2009; Wang et al., 2012;

63   Zhang et al., 2014). Zhang et al. (2014) have highlighted the importance of the

64   trans-boundary transport and the cooperation with neighboring provinces to control the O$_3$

65   level in Beijing. Pollutants transported from outside of Beijing and formed locally together

66   determine the air quality in Beijing (Meng et al., 2006; Zhang et al., 2012).

67   Several studies have been performed to investigate the role of trans-boundary transport

68   in the air quality of Beijing based on observational analysis and model simulations. Using the

69   US EPA's Model-3/CMAQ model simulation in the Beijing area, Streets et al. (2007) have

70   pointed out that non-Beijing sources can contribute 50-70% of Beijing's PM$_{2.5}$ concentration

71   and 20-30% of O$_3$ concentration. Wang et al. (2009) have indicated that O$_3$ formation in

72   Beijing is not only affected by local emissions, but also influenced by Tianjin and the south

73   of Hebei Province. The intense regional transport of pollutants from south to north in NCP

74   has been proposed to be the main reason for the heavy haze pollution in January 2013 in

75   Beijing (Sun et al., 2014; Tao et al., 2014; Wang et al., 2014b). Jiang et al. (2015) have

76   demonstrated that the transport from the environs of Beijing contributes about 55% of the

77   peak PM$_{2.5}$ concentration in the city during a heavy haze event in December 2013.

Atmospheric
Chemistry
and Physics
Discussions

78   Since September 2013, the 'Atmospheric Pollution Prevention and Control Action Plan'

79   (hereafter referred to as APPCAP) has been implemented, which is released by the Chinese

80   State Council to reduce $PM_{2.5}$ by up to 25% by 2017 relative to 2012 levels. After

81   implementation of the APPCAP, high $PM_{2.5}$ mass concentrations still can be observed and

82   the O_3 pollution has deteriorated during summertime since 2013 in Beijing (Chen et al., 2015;

83   Wang et al., 2016). Hence, studies are imperative to explore the O_3 and $PM_{2.5}$ formation from

84   various sources and evaluate the pollutants contributions from local production and

85   trans-boundary transport in Beijing, to support the design of mitigation strategies.

86   The purpose of the present study is to evaluate the contributions of trans-boundary

87   transport of emissions outside of Beijing to the air quality in Beijing and interaction of

88   emissions in and outside of Beijing using the WRF-CHEM model. The model configuration

89   and methodology are described in Section 2. Model results and sensitivity studies are

90   presented in Section 3, and conclusions and discussions are given in Section 4.

91

92   **2   Model and Methodology**

93   **2.1   WRF-CHEM Model**

94   The WRF-CHEM model used in the study is developed by Li et al. (2010, 2011a, b,

95   2012) at the Molina Center for Energy and the Environment, with a new flexible gas phase

96   chemical module and the CMAQ aerosol module developed by US EPA. The wet deposition

97   follows the method used in the CMAQ and the surface deposition of chemical species is

98   parameterized following Wesely (1989). The photolysis rates are calculated using the FTUV

99   (Li et al., 2005; Li et al., 2011a), in which the effects of aerosols and clouds on photolysis are

Atmospheric
Chemistry
and Physics
Discussions

Open Access

EGU

100   considered.

101   The inorganic aerosols are predicted in the WRF-CHEM model using ISORROPIA

102   Version 1.7 (Nenes et al., 1998). The secondary organic aerosol (SOA) formation is

103   calculated using a non-traditional SOA module. The volatility basis-set (VBS) modeling

104   method is used in the module, assuming that primary organic components are semi-volatile

105   and photochemically reactive and are distributed in logarithmically spaced volatility bins.

106   Detailed information about the volatility basis-set approach can be found in Li et al (2011b).

107   The SOA formation from glyoxal and methylglyoxal is also parameterized as a first-order

108   irreversible uptake by aerosol particles and cloud droplets.

109   **2.2   Model Configuration**

110   A persistent air pollution episode from 5 to 14 July 2015 in Beijing-Tianjin-Hebei

111   (BTH) is simulated using the WRF-CHEM model. During the episode, the observed mean

112   daily $PM_{2.5}$ concentration is 73.8 μg m^{-3} and the average O_3 concentration in the afternoon

113   reaches 237.0 μg m^{-3} in Beijing. The WRF-CHEM model adopts one grid with horizontal

114   resolution of 6 km and 35 sigma levels in the vertical direction, and the grid cells used for the

115   domain are 200 × 200 (Figure 1). The physical parameterizations include the microphysics

116   scheme of Hong et al (Hong and Lim, 2006), the Mellor, Yamada, and Janjic (MYJ) turbulent

117   kinetic energy (TKE) planetary boundary layer scheme (Janjić, 2002), the Unified Noah

118   land-surface model (Chen and Dudhia, 2001), the rapid radiative transfer model (RRTM)

119   long wave radiation scheme (Mlawer et al., 1997) and the Goddard shortwave

120   parameterization (Suarex and Chou, 1994). The NCEP 1° × 1° reanalysis data are used to

121   obtain the meteorological initial and boundary conditions. The chemical initial and boundary

Atmospheric
Chemistry
and Physics
Discussions

Open Access

EGU

122 conditions are interpolated from the 6h output of MOZART (Horowitz et al., 2003). The

123 spin-up time of the WRF-CHEM model is 28 hours. The SAPRC-99 (Statewide Air Pollution

124 Research Center, version 1999) chemical mechanism is used in the present study. The

125 anthropogenic emissions are developed by Zhang et al. (2009), including contributions from

126 agriculture, industry, power generation, residential, and transportation sources. The biogenic

127 emissions are calculated online using the MEGAN (Model of Emissions of Gases and

128 Aerosol from Nature) model developed by Guenther et al (2006).

129 **2.3   Factor Separation Approach**

130 The formation of the secondary atmospheric pollutant, such as O_3, secondary organic

131 aerosol, and nitrate, is a complicated nonlinear process in which its precursors from various

132 emission sources and transport react chemically or reach equilibrium thermodynamically.

133 Nevertheless, it is not straightforward to evaluate the contributions from different factors in a

134 nonlinear process. The factor separation approach (FSA) proposed by Stein et al. (1993) can

135 be used to isolate the effect of one single factor from a nonlinear process and has been widely

136 used to evaluate source effects (Gabusi et al., 2008; Weinroth et al., 2008; Carnevale et al.,

137 2010; Li et al., 2014). The total effect of one factor in the presence of others can be

138 decomposed into contributions from the factor and that from the interactions of all those

139 factors.

140 Suppose that field f depends on a factor φ:

141 $$f = f(\varphi)$$

142 The FSA decomposes function $f(\varphi)$ into a constant part that does not depend on φ ($f(0)$)

143 and a φ-depending component ($f'(\varphi)$), as follows:

Atmospheric
Chemistry
and Physics
Discussions

144 $f'(0) = f(0)$

145 $f'(\varphi) = f(\varphi) - f(0)$

146 Considering that there are two factors X and Y that influence the formation of secondary

147 pollutants in the atmosphere and also interact with each other. Denoting f_{XY}, f_X, f_Y, and

148 f_0 as the simulations including both of two factors, factor X only, factor Y only, and none of

149 the two factors, respectively. The pure contributions of factor X and Y can be isolated as

150 follows:

151 $f'_X = f_X - f_0$

152 $f'_Y = f_Y - f_0$

153 Note that term $f'_{X(Y)}$ represents the pure impacts of factor $X(Y)$, while f_0 is the term

154 independent of factors X and Y.

155 The simulation including both factors X and Y is given by:

156 $f_{XY} = f_0 + f'_X + f'_Y + f'_{XY}$

157 The mutual interaction between X and Y can be expressed as:

158 $f'_{XY} = f_{XY} - f_0 - f'_X - f'_Y = f_{XY} - (f_X - f_0) - (f_Y - f_0) - f_0 = f_{XY} - f_X - f_Y + f_0$

159 The above equation shows that the study needs four simulations, f_{XY}, f_X, f_Y and f_0, to

160 evaluate the contributions of two factors and their synergistic interactions.

161 **2.4 Statistical Methods for Comparisons**

162 In the present study, the mean bias (*MB*), root mean square error (*RMSE*) and the index

163 of agreement (*IOA*) are used as indicators to evaluate the performance of WRF-CEHM model

164 in simulation against measurements. *IOA* describes the relative difference between the model

165 and observation, ranging from 0 to 1, with 1 indicating perfect agreement.

Atmospheric
Chemistry
and Physics
Discussions

Open Access

EGU

166 $$MB = \frac{1}{N}\sum_{i=1}^{N}(P_i - O_i)$$

167 $$RMSE = \left[\frac{1}{N}\sum_{i=1}^{N}(P_i - O_i)^2\right]^{\frac{1}{2}}$$

168 $$IOA = 1 - \frac{\sum_{i=1}^{N}(P_i - O_i)^2}{\sum_{i=1}^{N}(|P_i - \overline{O}| + |O_i - \overline{O}|)^2}$$

169 where P_i and O_i are the predicted and observed pollutant concentrations, respectively. N is

170 the total number of the predictions used for comparisons, and $\overline{P}$ and $\overline{O}$ represents the

171 average of the prediction and observation, respectively.

172 **2.5 Pollutants Measurements**

173 The hourly measurements of O_3, NO_2, and $PM_{2.5}$ used in the study are downloaded

174 from the website http://www.aqistudy.cn/. The submicron sulfate, nitrate, ammonium, and

175 organic aerosols are observed by the Aerodyne Aerosol Chemical Speciation Monitor

176 (ACSM), which is deployed at the National Center for Nanoscience and Technology

177 (NCNST), Chinese Academy of Sciences, Beijing (Figure 1). The mass spectra of organic

178 aerosols are analyzed using the Positive Matrix Factorization (PMF) technique to separate

179 into four components: hydrocarbon-like organic aerosol (HOA)，cooking organic aerosol

180 (COA)，coal combustion organic aerosol (CCOA), and oxygenated organic aerosol (OOA).

181 HOA, COA, and CCOA are interpreted as surrogates of primary organic aerosol (POA), and

182 OOA is a surrogate of SOA.

183

184 **3 Results and Discussions**

185 **3.1 Summertime Air Quality in Beijing**

186 The APPCAP has been implemented since 2013 September, so comparisons of

187 summertime pollutants between 2013 and 2015 can show the mitigation effects on the air

Atmospheric
Chemistry
and Physics
Discussions

Open Access

EGU

188   quality. Considering that high O_3 concentrations generally take place in the afternoon during

189   summertime, Table 1 presents the summertime hourly concentrations of pollutants in the

190   afternoon (12:00 – 18:00 Beijing Time (BJT)) averaged at 12 monitoring sites in Beijing in

191   2013 and 2015. Apparently, implementation of the APPCAP has considerably decrease the

192   concentrations of primary species of CO and SO_2, particularly with regard to SO_2, reduced by

193   more than 40% from 2013 to 2015. Most of NO_x exist in the form of NO_2 in the afternoon

194   during summertime due to active photochemical processes. Therefore, 25.1% decrease of

195   NO_2 in the afternoon from 2013 to 2015 shows that the NO_x emission mitigation is also

196   effective in Beijing. The $PM_{2.5}$ concentrations are decreased by about 24.0% from 2013 to

197   2015, approaching the expected 25% reduction by 2017 relative to 2012 levels. However, the

198   O_3 trend is not anticipated in Beijing, and O_3 concentrations are increased from 133.0 µg m^{-3}

199   in 2013 to 163.2 µg m^{-3} in 2015, enhanced by 22.8%. For the discussion convenience, we

200   have defined the O_3 exceedance with hourly O_3 concentrations exceeding 200 µg m^{-3} and

201    $PM_{2.5}$ exceedance with hourly $PM_{2.5}$ concentrations exceeding 75 µg m^{-3}. Although the $PM_{2.5}$

202   exceedance frequency in the afternoon has been decreased by 25.0% from 2013 to 2015, but

203   still remains 32.7% in 2015. The O_3 exceedance frequency in 2015 is 31.8%, enhanced by

204   57.6% compared to 20.2% in 2013. Hence, during the summertime of 2015, two years after

205   implementation of the APPCAP, Beijing still has experienced high O_3 and/or $PM_{2.5}$

206   pollutions frequently.

207   **3.2   Model Performance**

208   The hourly measurements of O_3, NO_2, and $PM_{2.5}$ in Beijing-Tianjin-Hebei (BTH) and

209   ACSM measured aerosol species in Beijing are used to validate the WRF-CHEM model

210 simulations.

211 ### 3.2.1 O_3, NO_2, and $PM_{2.5}$ Simulations in Beijing

212 Figure 2 shows the temporal variations of observed and simulated near-surface O_3, NO_2,

213 and $PM_{2.5}$ concentrations averaged over monitoring sites in Beijing from 5 to 14 July 2015.

214 The WRF-CHEM model performs reasonably well in simulating the $PM_{2.5}$ variations

215 compared with observations in Beijing. The *MB* and *RMSE* are -3.6 μg m^{-3} and 22.5 μg m^{-3},

216 respectively, and the *IOA* is 0.86. The underestimation of $PM_{2.5}$ concentrations on July 8 and

217 overestimation on July 11 and 14 are still rather large, perhaps caused by the simulated wind

218 field uncertainties that influence the pollutants transports from outside of Beijing or lack of

219 resolving convective clouds due to the 6 km horizontal resolution. The model well

220 reproduces the temporal variations of O_3 concentrations, with an *IOA* of 0.92. The model

221 considerably underestimates the O_3 concentration during daytime on July 5, 6 and 13. Most

222 of monitoring sites in Beijing are concentrated in the urban area. Therefore, if the simulated

223 winds cause the O_3 plume formed in the urban area to leave early or deviate the O_3 plume

224 transported from outside of Beijing from the urban area, the model is subject to underestimate

225 the O_3 concentration in Beijing (Bei et al., 2010). The WRF-CHEM model also reasonably

226 yields the NO_2 diurnal profiles, but frequently overestimates the NO_2 concentrations during

227 nighttime, which is likely caused by the failure of boundary layer simulations.

228 ### 3.2.2 Aerosol Species Simulations in Beijing

229 Figure 3 shows the temporal variations of simulated and observed aerosol species at

230 NCNST site in Beijing from 5 to 14 July 2015. The WRF-CHEM model generally performs

231 reasonably in simulating the aerosol species variations compared with ACSM measurements.

Atmospheric
Chemistry
and Physics
Discussions

232   As a primary aerosol species, the POA in Beijing is determined by direct emissions from

233   various sources and transport from outside of Beijing, so uncertainties from emissions and

234   meteorological fields remarkably affect the model simulations (Bei et al., 2012;Bei et al.,

235   2013). Although the *MB* and *RMSE* for POA are 0.0 μg m^{-3} and 3.1 μg m^{-3}, respectively, the

236   *IOA* is less than 0.60, indicating the considerable biases in POA simulations. The

237   WRF-CHEM model has difficulties in well simulating the sulfate aerosol, with an *IOA* lower

238   than 0.60. The model cannot produce the observed high peaks of sulfate aerosols around

239   noontime on 8, 11, and 12 July 2015. The sulfate aerosol in the atmosphere is produced from

240   multiple sources, including SO_2 gas-phase oxidations by hydroxyl radicals (OH) and

241   stabilized criegee intermediates (sCI), aqueous reactions in cloud or fog droplets, and

242   heterogeneous reactions on aerosol surfaces, as well as direct emissions from power plants

243   and industries. There are two possible reasons for the biases in sulfate simulations. Firstly,

244   the model is not able to resolve well convective clouds due to the 6 km horizontal resolution

245   used in simulations, reducing the sulfate production from cloud processes. Secondly, a large

246   amount of SO_2 is released from point sources, such as power plants or agglomerated

247   industrial zones, and the transport of SO_2 from point sources is much sensitive to wind field

248   simulations. The model reasonably well reproduces the observed temporal variations of SOA,

249   nitrate, and ammonium, with *IOA*s exceeding 0.75.

250   **3.2.2 O_3, NO_2, and $PM_{2.5}$ Simulations in BTH**

251   Figure 4 shows the diurnal profiles of observed and simulated near-surface O_3, NO_2,

252   and $PM_{2.5}$ concentrations averaged over monitoring sites in BTH from 5 to 14 July 2015. The

253   WRF-CHEM model exhibits good performance in predicting the temporal variations of O_3,

Atmospheric
Chemistry
and Physics
Discussions

254   NO_2, and $PM_{2.5}$ concentrations compared with measurements in BTH, with *IOA*s higher than

255   0.80. In addition, O_3 and NO_2 simulations are also improved in BTH compared to those in

256   Beijing, indicating better model performance for regional simulations in a large scale.

257   Figure 5 presents the distributions of calculated and observed near-surface $PM_{2.5}$

258   concentrations along with the simulated wind fields at 10:00 Beijing Time (BJT) on the six

259   selected representative days with high O_3 and $PM_{2.5}$ concentrations. The calculated $PM_{2.5}$

260   spatial patterns generally agree well with the observations at the monitoring sites. The

261   observed $PM_{2.5}$ concentrations in BTH are still high even after implementation of the

262   APPCAP, frequently exceeding 75 µg m^{-3} on the selected six days. The $PM_{2.5}$ concentrations

263   in Beijing are higher than 115 µg m^{-3} at 10:00 BJT on 8, 11, and 12 July 2015, causing

264   moderate air pollution.

265   Further analyses are provided to interpret the high $PM_{2.5}$ formation in Beijing on July 8

266   and 11, 2015. Figure 6 presents the haze formation process from 20:00 BJT on July 7 to

267   18:00 BJT on July 8 in Beijing. From 20:00 to 22:00 on July 7, the prevailing southeast

268   winds bring the pollutants formed in Tianjin to Beijing. Meanwhile, a $PM_{2.5}$ plume in the east

269   of Beijing has been enhanced and commenced to be transported to Beijing. From 00:00 BJT

270   to 06:00 BJT on July 8, the formed $PM_{2.5}$ plume in the east of Beijing has been transported to

271   the city, but only partially influenced the urban area due to the prevailing northeast winds.

272   From 08:00 to 10:00 on July 8, the $PM_{2.5}$ pollution in the urban area of Beijing is enhanced

273   due to rush hour emissions. After 12:00 BJT on July 8, the $PM_{2.5}$ plume formed in the urban

274   area of Beijing has been transported to the northwest of Beijing and prevailing southeast

275   winds continuously carry the $PM_{2.5}$ formed in Tianjin to Beijing. Figure 7 shows the

Atmospheric
Chemistry
and Physics
Discussions

276   dominant role of trans-boundary transport in the haze formation in Beijing from 20:00 BJT

277   on July 10 to 18:00 BJT on July 11. From 20:00 on July 10 to 08:00 BJT on July 11, a $PM_{2.5}$

278   plume formed in the east of Beijing has been transported to Beijing forced by east winds,

279   causing continuous increase of the $PM_{2.5}$ concentration in Beijing. From 08:00 to 12:00 BJT

280   on July 11, the transported $PM_{2.5}$ plume from outside of Beijing has been further enhanced

281   due to rush hour emissions in Beijing, but the WRF-CHEM model overestimates the $PM_{2.5}$

282   concentration in the urban area due to the simulated weak or calm winds. After 12:00 BJT on

283   July 11, the enhanced south winds commence to transport the $PM_{2.5}$ plume in the urban area

284   to the north of Beijing.

285   The O_3 concentration during summertime reaches its peak during the period from 14:00

286   to 16:00 BJT in Beijing (Tang et al., 2012). Figure 8 presents the spatial distribution of

287   calculated and measured near-surface O_3 concentration at 15:00 Beijing Time (BJT) on the

288   selected six days, along with the simulated wind fields. In general, the simulated O_3 spatial

289   patterns are consistent with the measurements, but model biases still exist, possibly caused by

290   the active convections in the afternoon, which cannot be well resolved in WRF-CHEM model.

291   High O_3 concentrations at 15:00 BJT in Beijing are observed and also simulated by the model,

292   frequently exceeding 250 μg m^{-3}. The O_3 transport to Beijing from its surrounding areas is

293   also obvious when the winds are easterly or southerly. Figure 9 provides the spatial

294   distribution of simulated and observed near-surface NO_2 concentration on the selected six

295   days at 08:00 BJT when the NO_2 concentration reaches it peak due to rush hour NO_x

296   emissions and low planetary boundary layer (PBL). The simulated near-surface NO_2

297   concentrations highlights the dominant impact of the anthropogenic emissions, primarily

Atmospheric
Chemistry
and Physics
Discussions

Open Access

EGU

298   concentrated in cities or their downwind areas, which generally agree well with the

299   measurements. Beijing is surrounded from south to east by cities with high NO_2

300   concentrations, which can influence the O_3 formation in Beijing when south or east winds are

301   prevalent.

302   The good agreements between predicted $PM_{2.5}$, O_3, NO_x and aerosol species and the

303   corresponding measurements show that the modeled meteorological fields and emissions

304   used in simulations are generally reasonable.

305   **3.3   Contributions of Trans-boundary Transport to the O_3 and $PM_{2.5}$ Levels in Beijing**

306   The FSA is used in the present study to evaluate the contributions and interactions of

307   emissions from Beijing and outside of Beijing to the near-surface concentrations of O_3 and

308    $PM_{2.5}$ in Beijing. Four model simulations are performed, including f_{BS} with both the

309   anthropogenic emissions from Beijing and outside of Beijing, f_B with the emission from

310   Beijing alone, f_S with only emissions outside of Beijing, and f_0 without both the

311   emissions from Beijing and outside of Beijing, representing background concentrations. The

312   air pollutants levels in Beijing are determined by the contribution from pure local emissions

313   (f'_B, $f_B - f_0$), the trans-boundary transport of pure emissions outside of Beijing (f'_S,

314    $f_S - f_0$), emission interactions (f'_{BS}, $f_{BS} - f_B - f_S + f_0$), and the background (f_0).

315   Figure 10 provides the temporal variation of the average contributions to near-surface

316   O_3 and $PM_{2.5}$ concentrations in Beijing from total emissions (f_{BS}), emissions from Beijing

317   (f_B) and outside of Beijing (f_S) during the simulation episode. Apparently, the emissions

318   outside of Beijing generally play a more important role in the O_3 level of Beijing than the

319   Beijing local emissions. Even when the Beijing local emissions are excluded, the O_3

Atmospheric
Chemistry
and Physics
Discussions

320 concentration in Beijing still remains high level, with an average of 153 µg m^{-3} and ranging

321 from 130 to 180 µg m^{-3} in the afternoon. When only considering the Beijing local emission in

322 simulations, the afternoon average O_3 concentration in Beijing is approximately 126.6 µg m^{-3},

323 varying from 80 to 160 µg m^{-3}. On July 13, the contribution from Beijing local emissions

324 exceeds that from emissions outside of Beijing because north winds are prevailing, bringing

325 clean air to Beijing (Figure 8f). Table 2 gives the average O_3 contributions from 12:00 to

326 18:00 BJT in Beijing from pure Beijing local emissions, pure emissions outside of Beijing,

327 emission interactions, and background. The pure local emissions contribute about 22.4% on

328 average in the afternoon to the O_3 level in Beijing, varying from 15.5% to 35.4%. The pure

329 emissions outside of Beijing contribute more than pure local sources, with an average

330 contribution of 36.6%, ranging from 15.2% to 48.0%. The emission interactions in Beijing

331 decrease the O_3 level by 5.1% on average. O_3 formation is a nonlinear process, depending on

332 not only the absolute levels of NO_x and VOCs, but also the ratio of VOC_s/NO_x. When the O_3

333 precursors emitted from outside of Beijing are transported to Beijing and mixed with local

334 emissions, the concentrations of O_3 precursors are increased and the ratio of VOC_s/NO_x is

335 also altered, causing the formed O_3 concentration unequal to the simple linear summation of

336 O_3 contributions from the local and outside of Beijing emissions. The background O_3 in

337 Beijing plays an important role in the O_3 level in the afternoon, accounting for 45.6% of the

338 O_3 concentration. The O_3 contributions in Beijing induced by the trans-boundary transport of

339 emissions outside of Beijing is about 31.5% of the O_3 concentration during the study episodes,

340 indicating that the trans-boundary transport constitutes the main reason for the elevated O_3

341 level in Beijing after implementation of the APPCAP.

Atmospheric
Chemistry
and Physics
Discussions

342   When the Beijing local emissions are not considered in simulations, Beijing still

343   experiences high $PM_{2.5}$ pollution, with an average $PM_{2.5}$ concentration of 48.3 μg m^{-3} during

344   the simulation episode, and the $PM_{2.5}$ level in Beijing still exceeds 75 μg m^{-3} on several days.

345   However, when only considering the Beijing local emissions, the average $PM_{2.5}$

346   concentration in Beijing is 19.6 μg m^{-3} during the episode, showing that Beijing's $PM_{2.5}$

347   pollution is dominated by the trans-boundary transport. During the study episode, the average

348    $PM_{2.5}$ contribution from the pure local emissions is 13.7%, which is much lower than the

349   contribution of 61.5% from the pure emissions outside of Beijing, further showing the

350   dominant role of the trans-boundary transport in the Beijing $PM_{2.5}$ pollution. The emission

351   interactions enhance the $PM_{2.5}$ level in Beijing on average, with a contribution of 5.9%. The

352   background $PM_{2.5}$ contribution to Beijing is 18.9% on average, lower than those for O_3. The

353    $PM_{2.5}$ contributions caused by the trans-boundary transport is about 67.4% of $PM_{2.5}$

354   concentrations in Beijing, indicating that the cooperation with neighboring provinces to

355   control the $PM_{2.5}$ level is a key for Beijing to improve air quality.

356   Figure 11 shows the temporal variation of the averaged contributions to the near-surface

357   aerosol constituents from total emissions (f_{BS}), pure emissions from Beijing (f'_B), the

358   trans-boundary transport of pure emissions outside of Beijing (f'_S), emission interactions

359   (f'_{BS}), and the background (f_0) during the simulation episode. The temporal variations of

360   elemental carbon (EC) and POA from pure local emissions and trans-boundary transport

361   exhibit obvious diurnal cycles, e.g., highest during nighttime and lowest in the afternoon,

362   corresponding to the variations of PBL height and anthropogenic emissions. The SOA from

363   pure local emissions reaches its peak in the afternoon when the O_3 concentration is high, but

Atmospheric
Chemistry
and Physics

Open Access

Discussions

EGU

364   the trans-boundary transport causes the gradual accumulation process of SOA in Beijing from

365   July 5 to 9 and from July 9 to 13. The sulfate temporal profile from the trans-boundary

366   transport is similar to that of SOA, also showing the accumulation process. In addition, the

367   sulfate aerosols from pure local emissions do not vary remarkably. The nitrate aerosols from

368   pure local emissions and the trans-boundary transport generally attain peaks in the morning

369   when the air temperature is not high and the HNO_3 concentrations are not low. The

370   ammonium aerosol variations are generally determined by those of sulfate and nitrate

371   aerosols. For example, the variations of ammonium aerosols from the trans-boundary include

372   not only the morning peaks, but also the accumulation processes from July 5 to 9 and from

373   July 9 to 13. Except the sulfate aerosol, the temporal variations of aerosol species from

374   background are not large.

375   Table 4 presents the average aerosol constituents contributions from pure Beijing local

376   emissions, pure emissions outside of Beijing, emission interactions, and the background, and

377   mass fractions in the total $PM_{2.5}$ in Beijing during the episode. Organic aerosols (POA+SOA)

378   constitute the most important component of $PM_{2.5}$, accounting for 34.8% of $PM_{2.5}$ mass

379   concentration, which is consistent with the ACSM measurement in Beijing (Sun et al., 2014).

380   In addition, SOA contributes more than 70% of organic aerosol mass concentrations, which is

381   due to the high atmospheric oxidation capability caused by elevated O_3 concentrations during

382   summertime. Although the SO_2 concentrations have been decreased by more than 40% since

383   implementation of the APPCAP, sulfate aerosols still play an important role in the $PM_{2.5}$

384   level in Beijing and make up 25.1% of the $PM_{2.5}$ mass concentrations, showing high sulfate

385   contributions from the trans-boundary transport and background. The ammonium, nitrate, EC,

386   and unspecified species account for 13.7%, 14.1%, 5.8%, and 6.5% of the $PM_{2.5}$ mass

387   concentrations, respectively. Secondary aerosol species dominate the $PM_{2.5}$ mass

388   concentration in Beijing, with a contribution of 77.9%, corresponding to the high atmospheric

389   oxidation capability.

390   The pure local emissions contribute more than 20% of the mass concentrations for the

391   primary aerosol species, but less than 15% for the secondary aerosol species in Beijing (Table

392   4). The trans-boundary transport of emissions outside of Beijing dominates all the aerosol

393   species levels in Beijing, with contributions exceeding 50%, particularly for SOA and nitrate.

394   In addition, the POA and sulfate background contributions are also high, more than 20%.

395   Although the primary aerosol species of EC and unspecified constituents are not involved in

396   the chemical process and also do not participate the gas-particle partitioning, the emission

397   interactions still enhance EC and unspecified constituents concentrations, with contributions

398   of around 1.5%, which is caused by the aerosol radiative effect. Mixing of Beijing local

399   emissions with those outside of Beijing increases the aerosol concentrations in the PBL and

400   decreases the incoming solar radiation down to the surface, cooling the temperature of the

401   low level atmosphere to suppress the development of PBL and hinder the aerosol dispersion

402   in the vertical direction. The emission interactions increase the POA and SOA concentrations,

403   with a POA contribution of 5.3% and a SOA contribution of 5.9%. In the VBS modeling

404   approach, primary organic components are assumed to be semi-volatile and photochemically

405   reactive. Mixing of Beijing local emissions with emissions outside of Beijing enhances the

406   organic condensable gases, and considering that the saturation concentrations of the organic

407   condensable gases do not change, more organic condensable gases participate into the

Atmospheric
Chemistry
and Physics
Discussions

408   particle phase, increasing the POA and SOA concentrations. The contributions of emission

409   interactions to inorganic aerosols, including sulfate, nitrate, and ammonium, are more

410   complicated, depending on their particle phase and precursors concentrations. In the present

411   study, ISORROPIA (Version 1.7) is used to calculate the thermodynamic equilibrium

412   between the sulfate-nitrate-ammonium-water aerosols and their gas phase precursors

413   H_2SO_4-HNO_3-NH_3-water vapor. Although mixing of Beijing local emissions with those

414   outside of Beijing increase inorganic aerosols precursors, the inorganic aerosol contributions

415   from emission interactions are still uncertain due to the deliberate thermodynamic

416   equilibrium between inorganic aerosols and their precursors. High atmospheric oxidation

417   capability induced by elevated O_3 concentration facilitates HNO_3 formation through NO_2

418   reaction with OH during daytime and N_2O_5 formation through NO_2 reaction with O_3 during

419   nighttime. High O_3 concentrations are produced by Beijing local emissions and those outside

420   of Beijing, accelerating the HNO_3 or N_2O_5 formation. Hence, mixing of Beijing local

421   emissions with those outside of Beijing considerably increases the HNO_3 or N_2O_5 levels,

422   pushing more HNO_3 or N_2O_5 into the particle phase. The nitrate contributions from emission

423   interactions are 18.1%, much more than those for other aerosol constituents. SO_2 gas-phase

424   oxidations by OH and sCI are not as fast as NO_2 reaction with OH, so the formation of

425   sulfuric acid is slow, although the O_3 concentration is high during summertime. Therefore,

426   the sulfate contributions from emission interactions is not significant, only 3.4%. As the

427   ammonium precursor, NH_3 is generally from direct emissions. The ammonium contributions

428   from emission interactions are 1.5%, similar to those of primary aerosol species that are

429   caused by aerosol radiative effects, indicating that the NH_3 emissions are not sufficiently high

Atmospheric
Chemistry
and Physics
Discussions
Open Access
EGU

430   in Beijing and outside of Beijing.

431

432   **4   Summary and Conclusions**

433   In the present study, a persistent air pollution episode with high concentrations of O_3

434   and $PM_{2.5}$ are simulated using the WRF-CHEM model during the period from July 5 to 14,

435   2015 in BTH, to evaluate the contributions of trans-boundary transport to the air quality in

436   Beijing. Although the APPCAP has been implemented since 2013 September, the average O_3

437   concentration in the afternoon has been increased by 22.8% from 2013 to 2015 in Beijing,

438   and Beijing still has experienced high O_3 and/or $PM_{2.5}$ pollutions frequently during

439   summertime of 2015.

440   In general, the predicted temporal variations of $PM_{2.5}$, O_3, and NO_2 concentrations agree

441   well with observations in Beijing and BTH, but the model biases still exist, which is perhaps

442   caused by the uncertainties of simulated meteorological conditions and the emission

443   inventory. The model also successfully reproduces the spatial distributions of $PM_{2.5}$, O_3, and

444   NO_2 concentrations compared with measurements. The model performs reasonably well in

445   modeling the variations of aerosol constituents compared with ACSM measurement at

446   NCNST site in Beijing, but there are considerable biases in POA and sulfate simulations.

447   The FSA is used to investigate the contribution of trans-boundary transport of emissions

448   outside of Beijing to the air quality in Beijing. If the Beijing local emissions are not

449   considered in model simulations, the O_3 and $PM_{2.5}$ concentrations in Beijing still remain high

450   levels, showing that the trans-boundary transport of emissions outside of Beijing plays a

451   more important role in the air quality in Beijing than the Beijing local emissions. On average,

Atmospheric
Chemistry
and Physics
Discussions

452   the pure Beijing local emissions contribute 22.4% of O_3 in the afternoon and 13.7% of $PM_{2.5}$

453   mass concentrations in Beijing during the episode. The O_3 contribution in the afternoon and

454     $PM_{2.5}$ contribution from the trans-boundary transport of emissions outside of Beijing are 36.6%

455   and 61.5%, respectively, far exceeding those from the pure local emissions. The interactions

456   of Beijing local emissions with those outside of Beijing generally decrease the O_3 level in the

457   afternoon and increase the $PM_{2.5}$ level in Beijing during the episode, with contributions of

458   -5.1% and +4.4%, respectively. In addition, the trans-boundary transport dominates all the

459   aerosol species levels in Beijing, with contributions exceeding 50% on average, particularly

460   for SOA and nitrate. The emission interactions in general increase all the aerosol species

461   levels due to the aerosol radiative effect and the enhancement of precursors of secondary

462   aerosols. Hence, the air quality in Beijing during summertime is principally determined by

463   the trans-boundary transport of emissions outside of Beijing. The cooperation with

464   neighboring provinces to decrease pollutant emissions is the optimum approach to mitigate

465   the air pollution in Beijing.

466   It is worth noting that, although the WRF-CHEM model well captures the spatial

467   distributions and temporal variations of pollutants, the model biases still exist. The

468   discrepancies between the predictions and observations are possibly caused by the

469   uncertainties in the emission inventory and the meteorological fields simulations. Future

470   studies need to be conducted to improve the WRF-CHEM model simulations, and further to

471   assess the contributions of trans-boundary transport of emissions outside of Beijing to the air

472   quality in Beijing, considering the rapid changes in anthropogenic emissions since

473   implementation of the APPCAP.

Atmospheric
Chemistry
and Physics
Discussions

Open Access

474

475 Data availability: The real-time O_3 and $PM_{2.5}$ are accessible for the public on the website

476 http://106.37.208.233:20035/. One can also access the historic profile of observed ambient

477 pollutants through visiting http://www.aqistudy.cn/.

478

484
485
486
487

Atmospheric
Chemistry
and Physics
Discussions

Reference

488

489   Bei, N., Lei, W., Zavala, M., and Molina, L. T.: Ozone predictabilities due to meteorological
490   uncertainties in the Mexico City basin using ensemble forecasts, Atmospheric Chemistry
491   and Physics, 10, 6295-6309, 10.5194/acp-10-6295-2010, 2010.

492   Bei, N., Li, G., and Molina, L. T.: Uncertainties in SOA simulations due to meteorological
493   uncertainties in Mexico City during MILAGRO-2006 field campaign, Atmospheric
494   Chemistry and Physics, 12, 11295-11308, 10.5194/acp-12-11295-2012, 2012.

495   Bei, N. F., Li, G. H., Zavala, M., Barrera, H., Torres, R., Grutter, M., Gutierrez, W., Garcia,
496   M., Ruiz-Suarez, L. G., Ortinez, A., Guitierrez, Y., Alvarado, C., Flores, I., and Molina, L.
497   T.: Meteorological overview and plume transport patterns during Cal-Mex 2010,
498   Atmospheric Environment, 70, 477-489, 10.1016/j.atmosenv.2012.01.065, 2013.

499   Carnevale, C., Pisoni, E., and Volta, M.: A non-linear analysis to detect the origin of PM10
500   concentrations in Northern Italy, Science of Total Environment, 409, 182-191,
501   http://dx.doi.org/10.1016/j.scitotenv.2010.09.038, 2010.

502   Chen, F., and Dudhia, J.: Coupling an advanced land surface-hydrology model with the Penn
503   State-NCAR MM5 modeling system. Part I: Model implementation and sensitivity, Mon.
504   Weather Rev., 129, 569-585, 10.1175/1520-0493(2001)129<0569:caalsh>2.0.co;2, 2001.

505   Chen, W., Yan, L., and Zhao, H. M.: Seasonal Variations of Atmospheric Pollution and Air
506   Quality in Beijing, Atmosphere, 6, 1753-1770, 10.3390/atmos6111753, 2015.

507   Gabusi, V., Pisoni, E., and Volta, M.: Factor separation in air quality simulations, Ecological
508   Modelling, 218, 383-392, http://dx.doi.org/10.1016/j.ecolmodel.2008.07.030, 2008.

509   Guenther, A., Karl, T., Harley, P., Wiedinmyer, C., Palmer, P. I., and Geron, C.: Estimates of
510   global terrestrial isoprene emissions using MEGAN (Model of Emissions of Gases and
511   Aerosols from Nature), Atmospheric Chemistry and Physics, 6, 3181-3210, 2006.

512   Hong, S.-Y., and Lim, J.-O. J.: The WRF Single-Moment 6-Class Microphysics Scheme
513   (WSM6), Asia-Pacific Journal of Atmospheric Sciences, 42, 129-151, 2006.

514   Horowitz, L. W., Walters, S., Mauzerall, D. L., Emmons, L. K., Rasch, P. J., Granier, C., Tie,
515   X. X., Lamarque, J. F., Schultz, M. G., Tyndall, G. S., Orlando, J. J., and Brasseur, G. P.:
516   A global simulation of tropospheric ozone and related tracers: Description and evaluation
517   of MOZART, version 2, Journal of Geophysical Research-Atmospheres, 108, 29,
518   10.1029/2002jd002853, 2003.

519   Huang, J., Liu, H., Crawford, J. H., Chan, C., Considine, D. B., Zhang, Y., Zheng, X., Zhao,
520   C., Thouret, V., Oltmans, S. J., Liu, S. C., Jones, D. B. A., Steenrod, S. D., and Damon,
521   M. R.: Origin of springtime ozone enhancements in the lower troposphere over Beijing:
522   in situ measurements and model analysis, Atmospheric Chemistry and Physics, 15,
523   5161-5179, 10.5194/acp-15-5161-2015, 2015.

524   Janjić, Z. I.: Nonsingular Implementation of the Mellor–Yamada Level 2.5 Scheme in the
525   NCEP Meso Model, Ncep Office Note, 436, 2002.

526   Jiang, C., Wang, H., Zhao, T., Li, T., and Che, H.: Modeling study of $PM_{2.5}$ pollutant

Atmospheric
Chemistry
and Physics
Discussions

527   transport across cities in China's Jing-Jin-Ji region during a severe haze episode in
528   December 2013, Atmospheric Chemistry and Physics, 15, 5803-5814,
529   10.5194/acp-15-5803-2015, 2015.

530 Jin, X. M., and Holloway, T.: Spatial and temporal variability of ozone sensitivity over China
531   observed from the Ozone Monitoring Instrument, Journal of Geophysical
532   Research-Atmospheres, 120, 7229-7246, 10.1002/2015jd023250, 2015.

533 Lei, W., de Foy, B., Zavala, M., Volkamer, R., and Molina, L. T.: Characterizing ozone
534   production in the Mexico City Metropolitan Area: a case study using a chemical transport
535   model, Atmospheric Chemistry and Physics, 7, 1347-1366, 2007.

536 Lei, W., Zavala, M., de Foy, B., Volkamer, R., and Molina, L. T.: Characterizing ozone
537   production and response under different meteorological conditions in Mexico City,
538   Atmospheric Chemistry and Physics, 8, 7571-7581, 2008.

539 Long, X., Tie, X., Cao, J., Huang, J., Feng, T., Li, N., Zhao, S., Tian, J., Li, G., and Zhang, Q.:
540   Impact of crop field burning and mountains on heavy haze in the North China Plain: a
541   case study, Atmospheric Chemistry and Physics, 16, 9675-9691,
542   doi:10.5194/acp-16-9675-2016, 2016.

543 Li, G., Zhang, R., Fan, J., and Tie, X.: Impacts of black carbon aerosol on photolysis and
544   ozone, Journal of Geophysical Research, 110, 10.1029/2005jd005898, 2005.

545 Li, G., Zhang, R., Fan, J., and Tie, X.: Impacts of biogenic emissions on photochemical
546   ozone production in Houston, Texas, Journal of Geophysical Research, 112,
547   10.1029/2006jd007924, 2007.

548 Li, G., Lei, W., Zavala, M., Volkamer, R., Dusanter, S., Stevens, P., and Molina, L. T.:
549   Impacts of HONO sources on the photochemistry in Mexico City during the
550   MCMA-2006/MILAGO Campaign, Atmospheric Chemistry and Physics, 10, 6551-6567,
551   10.5194/acp-10-6551-2010, 2010.

552 Li, G., Bei, N., Tie, X., and Molina, L. T.: Aerosol effects on the photochemistry in Mexico
553   City during MCMA-2006/MILAGRO campaign, Atmospheric Chemistry and Physics, 11,
554   5169-5182, 10.5194/acp-11-5169-2011, 2011a.

555 Li, G., Zavala, M., Lei, W., Tsimpidi, A. P., Karydis, V. A., Pandis, S. N., Canagaratna, M.
556   R., and Molina, L. T.: Simulations of organic aerosol concentrations in Mexico City using
557   the WRF-CHEM model during the MCMA-2006/MILAGRO campaign, Atmospheric
558   Chemistry and Physics, 11, 3789-3809, 10.5194/acp-11-3789-2011, 2011b.

559 Li, G. H., Bei, N. F., Zavala, M., and Molina, L. T.: Ozone formation along the California
560   Mexican border region during Cal-Mex 2010 field campaign, Atmospheric Environment,
561   88, 370-389, 10.1016/j.atmosenv.2013.11.067, 2014.

562 Li, R. K., Li, Z. P., Gao, W. J., Ding, W. J., Xu, Q., and Song, X. F.: Diurnal, seasonal, and
563   spatial variation of $PM_{2.5}$ in Beijing, Chinese Science Bulletin, 60, 387-395,
564   10.1007/s11434-014-0607-9, 2015a.

565 Li, X., Zhang, Q., Zhang, Y., Zheng, B., Wang, K., Chen, Y., Wallington, T. J., Han, W. J.,
566   Shen, W., Zhang, X. Y., and He, K. B.: Source contributions of urban $PM_{2.5}$ in the

Atmospheric
Chemistry
and Physics
Discussions

567 Beijing-Tianjin-Hebei region: Changes between 2006 and 2013 and relative impacts of
568 emissions and meteorology, Atmospheric Environment, 123, 229-239,
569 10.1016/j.atmosenv.2015.10.048, 2015b.

570 Liu, Z. R., Hu, B., Wang, L. L., Wu, F. K., Gao, W. K., and Wang, Y. S.: Seasonal and
571 diurnal variation in particulate matter (PM_{10} and $PM_{2.5}$) at an urban site of Beijing:
572 analyses from a 9-year study, Environmental Science and Pollution Research, 22,
573 627-642, 10.1007/s11356-014-3347-0, 2015.

574 Meng, W., Gao, Q., Zhang, Z., Liao, Q., Lei, t., Li, J., Kang, N., and Ren, Z.: The Numerical
575 Study of Atmospheric Pollution in Beijing and Its Surrounding Regions, Research of
576 Environmental Sciences, 19, 11-18, 2006.

577 Nenes, A., Pilinis, C., Pandis, S. N.: ISORROPIA: A New thermodynamic equilibrium model
578 for multiphase multicomponent inorganic aerosols, Aquatic Geochemistry, 4(1), 123-152,
579 http://nenes.eas.gatech.edu/ISORROPIA/, 1998.

580 Mlawer, E. J., Taubman, S. J., Brown, P. D., Iacono, M. J., and Clough, S. A.: Radiative
581 transfer for inhomogeneous atmospheres: RRTM, a validated correlated-k model for the
582 longwave, Journal of Geophysical Research-Atmosphere, 102, 16663-16682,
583 10.1029/97jd00237, 1997.

584 Parrish, D. and Zhu, T.: Clean air for Megacities, Science, 326, 674-675, 2009.

585 Putaud, J. P., Raes, F., Van Dingenen, R., Bruggemann, E., Facchini, M. C., Decesari, S.,
586 Fuzzi, S., Gehrig, R., Huglin, C., Laj, P., Lorbeer, G., Maenhaut, W., Mihalopoulos, N.,
587 Mulller, K., Querol, X., Rodriguez, S., Schneider, J., Spindler, G., ten Brink, H., Torseth,
588 K., and Wiedensohler, A.: European aerosol phenomenology-2: chemical characteristics
589 of particulate matter at kerbside, urban, rural and background sites in Europe,
590 Atmospheric Environment, 38, 2579-2595, 10.1016/j.atmosenv.2004.01.041, 2004.

591 Schwab, J. J., Felton, H. D., and Demerjian, K. L.: Aerosol chemical composition in New
592 York state from integrated filter samples: Urban/rural and seasonal contrasts, Journal of
593 Geophysical Research-Atmospheres, 109, 13, 10.1029/2003jd004078, 2004.

594 Sillman, S., Logan, J. A., and Wofsy, S. C.: The sensitivity of ozone to nitrogen oxides and
595 hydrocarbons in regional ozone episode, Journal of Geophysical Research-Atmospheres,
596 95, 1837-1851, 10.1029/JD095iD02p01837, 1990.

597 Stein, U., and Alpert, P.: Factor Seperation in numerical simulations, Journal of Atmospheric
598 Sciences, 50, 2107-2115, 10.1175/1520-0469(1993)050<2107:fsins>2.0.co;2, 1993.

599 Streets, D. G., Fu, J. S., Jang, C. J., Hao, J. M., He, K. B., Tang, X. Y., Zhang, Y. H., Wang,
600 Z. F., Li, Z. P., Zhang, Q., Wang, L. T., Wang, B. Y., and Yu, C.: Air quality during the
601 2008 Beijing Olympic Games, Atmospheric Environment, 41, 480-492,
602 10.1016/j.atmosenv.2006.08.046, 2007.

603 Suarex, M. J., and Chou, M. D.: Technical report series on global modeling and data
604 assimilation. Volume 3: An efficient thermal infrared radiation parameterization for use
605 in general circulation models, 1603-1609, 1994.

606 Sun, Y. L., Jiang, Q., Wang, Z. F., Fu, P. Q., Li, J., Yang, T., and Yin, Y.: Investigation of

Atmospheric
Chemistry
and Physics
Discussions

607   the sources and evolution processes of severe haze pollution in Beijing in January 2013,
608   Journal of Geophysical Research-Atmospheres, 119, 4380-4398, 10.1002/2014jd021641,
609   2014.

610 Tang, G., Li, X., Wang, Y., Xin, J., and Ren, X.: Surface ozone trend details and
611   interpretations in Beijing, 2001-2006, Atmospheric Chemistry and Physics, 9, 8813-8823,
612   2009.

613 Tang, G., Wang, Y., Li, X., Ji, D., Hsu, S., and Gao, X.: Spatial-temporal variations in
614   surface ozone in Northern China as observed during 2009-2010 and possible implications
615   for future air quality control strategies, Atmospheric Chemistry and Physics, 12,
616   2757-2776, 10.5194/acp-12-2757-2012, 2012.

617 Tao, M. H., Chen, L. F., Xiong, X. Z., Zhang, M. G., Ma, P. F., Tao, J. H., and Wang, Z. F.:
618   Formation process of the widespread extreme haze pollution over northern China in
619   January 2013: Implications for regional air quality and climate, Atmospheric
620   Environment, 98, 417-425, 10.1016/j.atmosenv.2014.09.026, 2014.

621 Wang, X. S., Li, J. L., Zhang, Y. H., Xie, S. D., and Tang, X. Y.: Ozone source attribution
622   during a severe photochemical smog episode in Beijing, China, Science of China Series B
623   - Chemistry, 52, 1270-1280, 10.1007/s11426-009-0137-5, 2009.

624 Wang, L. T., Wei, Z., Yang, J., Zhang, Y., Zhang, F. F., Su, J., Meng, C. C., and Zhang, Q.:
625   The 2013 severe haze over southern Hebei, China: model evaluation, source
626   apportionment, and policy implications, Atmospheric Chemistry and Physics, 14,
627   3151-3173, 10.5194/acp-14-3151-2014, 2014a.

628 Wang, Y., Konopka, P., Liu, Y., Chen, H., Muller, R., Ploger, F., Riese, M., Cai, Z., and Lu,
629   D.: Tropospheric ozone trend over Beijing from 2002-2010: ozonesonde measurements
630   and modeling analysis, Atmospheric Chemistry and Physics, 12, 8389-8399,
631   10.5194/acp-12-8389-2012, 2012.

632 Wang, Y. H., Hu, B., Tang, G. Q., Ji, D. S., Zhang, H. X., Bai, J. H., Wang, X. K., and Wang,
633   Y. S.: Characteristics of ozone and its precursors in Northern China: A comparative study
634   of three sites, Atmospheric Research, 132, 450-459, 10.1016/j.atmosres.2013.04.005,
635   2013.

636 Wang, Z., Li, Y., Chen, T., Zhang, D., Sun, F., Wang, X., Huan, N., and Pan, L.: Analysis on
637   diurnal variation characteristics of ozone and correlations with its precursors in urban
638   atmosphere of Beijing, China Environmental Science, 34, 3001-3008, 2014b.

639 Wang, Z., Zhang, D., Li, Y., Dong, X., Sun, R., and Sun, N.: Different Air Pollution
640   Situations of O_3 and $PM_{2.5}$ During Summer in Beijing, Environmental Science, 37,
641   807-815, 2016.

642 Weinroth, E., Luria, M., Emery, C., Ben-Nun, A., Bornstein, R., Kaplan, J., Peleg, M., and
643   Mahrer, Y.: Simulations of Mideast transboundary ozone transport: A source
644   apportionment case study, Atmospheric Environment, 42, 3700-3716,
645   10.1016/j.atmosenv.2008.01.002, 2008.

646 Wesely, M. L.: Parameterization of surface resistances to gaseous dry deposition in

Atmospheric
Chemistry
and Physics
Discussions

Open Access

647 regional-scale numerical models, Atmospheric Environment, 23, 1293-1304,
648   10.1016/0004-6981(89)90153-4, 1989.

649 Xie, Y. Y., Wang, Y. X., Zhang, K., Dong, W. H., Lv, B. L., and Bai, Y. Q.: Daily
650   Estimation of Ground-Level $PM_{2.5}$ Concentrations over Beijing Using 3 km Resolution
651   MODIS AOD, Environmental science & technology, 49, 12280-12288,
652   10.1021/acs.est.5b01413, 2015.

653 Xu, J., Zhang, Y. H., Fu, J. S., Zheng, S. Q., and Wang, W.: Process analysis of typical
654   summertime ozone episodes over the Beijing area, Science of Total Environment, 399,
655   147-157, 10.1016/j.scitotenv.2008.02.013, 2008.

656 Xu, J., Ma, J. Z., Zhang, X. L., Xu, X. B., Xu, X. F., Lin, W. L., Wang, Y., Meng, W., and
657   Ma, Z. Q.: Measurements of ozone and its precursors in Beijing during summertime:
658   impact of urban plumes on ozone pollution in downwind rural areas, Atmospheric
659   Chemistry and Physics, 11, 12241-12252, 10.5194/acp-11-12241-2011, 2011.

660 Zhang, R., Jing, J., Tao, J., Hsu, S.-C., Wang, G., Cao, J., Lee, C. S. L., Zhu, L., Chen, Z.,
661   Zhao, Y., and Shen, Z.: Chemical characterization and source apportionment of $PM_{2.5}$ in
662   Beijing: seasonal perspective, Atmospheric Chemistry and Physics, 13, 7053-7074,
663   doi:10.5194/acp-13-7053-2013, 2013.

664 Zhang, J. P., Zhu, T., Zhang, Q. H., Li, C. C., Shu, H. L., Ying, Y., Dai, Z. P., Wang, X., Liu,
665   X. Y., Liang, A. M., Shen, H. X., and Yi, B. Q.: The impact of circulation patterns on
666   regional transport pathways and air quality over Beijing and its surroundings,
667   Atmospheric Chemistry and Physics, 12, 5031-5053, 10.5194/acp-12-5031-2012, 2012.

668 Zhang, Q., Streets, D. G., Carmichael, G. R., He, K. B., Huo, H., Kannari, A., Klimont, Z.,
669   Park, I. S., Reddy, S., Fu, J. S., Chen, D., Duan, L., Lei, Y., Wang, L. T., and Yao, Z. L.:
670   Asian emissions in 2006 for the NASA INTEX-B mission, Atmospheric Chemistry and
671   Physics, 9, 5131-5153, 2009.

672 Zhang, Q., Yuan, B., Shao, M., Wang, X., Lu, S., Lu, K., Wang, M., Chen, L., Chang, C. C.,
673   and Liu, S. C.: Variations of ground-level O-3 and its precursors in Beijing in
674   summertime between 2005 and 2011, Atmospheric Chemistry and Physics, 14,
675   6089-6101, 10.5194/acp-14-6089-2014, 2014.

676 Zheng, S., Pozzer, A., Cao, C. X., and Lelieveld, J.: Long-term (2001-2012) concentrations
677   of fine particulate matter ($PM_{2.5}$) and the impact on human health in Beijing, China,
678   Atmospheric Chemistry and Physics, 15, 5715-5725, 10.5194/acp-15-5715-2015, 2015.

679

680

681

682

683

684   Table 1 Hourly mass concentrations of pollutants averaged in the afternoon at 12

685   monitoring sites in Beijing during summertime of 2013 and 2015.

Pollutants	CO (mg m^{-3})	SO$_2$ (μg m^{-3})	NO$_2$ (μg m^{-3})	O$_3$ (μg m^{-3})	PM$_{2.5}$ (μg m^{-3})
2013	1.09	9.85	31.6	133.0	81.4
2015	0.88	5.71	23.6	163.2	61.9
Change (%)	-20.0	-42.0	-25.1	+22.8	-24.0

686

687

688

689

690

Atmospheric
Chemistry
and Physics
Discussions

691 Table 2 Average O_3 contributions (%) from 12：00 to 18:00 BJT in Beijing from pure Beijing local
692 emissions, pure emissions outside of Beijing, the interactions of both emissions, and background from
693 5 to 14 July 2015.

694

Emissions	Beijing	Surroundings	Interactions	Background
Date	f'_B	f'_S	f'_{BS}	f_0
5	15.5	26.1	-2.4	60.8
6	19.8	30.9	-3.0	52.3
7	25.5	36.0	-3.6	42.1
8	27.0	36.9	-5.9	42.0
9	23.2	35.3	-4.6	46.1
10	18.6	39.9	-2.6	44.1
11	29.4	48.0	-10.0	32.6
12	35.4	40.6	-11.4	35.4
13	23.4	15.2	-1.5	62.9
14	20.3	32.2	-3.3	50.8
Average	22.4	36.6	-5.1	46.1

695
696
697
698
699

Atmospheric
Chemistry
and Physics
Discussions

700 Table 3 Average PM$_{2.5}$ contributions (%) in Beijing from pure Beijing local emissions, pure emissions
701 outside of Beijing, the interactions of both emissions, and background from 5 to 14 July 2015.
702

Emissions	Beijing	Surroundings	Interactions	Background
Date	f'_B	f'_S	f'_{BS}	f_0
5	14.6	55.1	3.3	27.0
6	14.9	56.3	3.4	25.4
7	14.2	56.4	8.0	21.4
8	13.2	61.1	6.4	19.3
9	15.3	61.3	6.3	17.1
10	11.5	66.5	6.2	15.8
11	9.7	71.0	8.1	11.2
12	14.2	67.6	5.6	12.6
13	19.2	47.2	3.6	30.0
14	16.6	53.1	6.4	23.9
Average	13.7	61.5	5.9	18.9

703
704
705
706

Atmospheric
Chemistry
and Physics
Discussions

707 Table 4 Aerosol species' contributions (%) from pure Beijing local emissions, pure emissions outside
708 of Beijing, interactions of both emissions, and background, and mass fraction in the total PM$_{2.5}$ (%) in
709 Beijing averaged during the period from 5 to 14 July 2015.
710

Emissions	Mass Fraction	Beijing	Surroundings	Interactions	Background
Species	In Total PM$_{2.5}$	f'_B	f'_S	f'_{BS}	f_0
EC	5.8	27.0	57.9	1.5	13.6
POA	9.8	20.8	49.0	5.3	24.9
SOA	25.0	14.6	64.2	5.9	15.3
Ammonium	13.7	14.5	65.7	1.5	18.3
Nitrate	14.1	10.1	71.7	18.1	0.1
Sulfate	25.1	6.5	52.9	3.4	37.2
Unspecified	6.5	21.2	61.4	1.6	15.8

711
712
713
714

Atmospheric
Chemistry
and Physics
Discussions

Open Access

Figure Captions

715

716

717   Figure 1 WRF-CHEM simulation domain. The blue circles represent centers of cities with

718   ambient monitoring sites and the red circle denotes the NCNST site. The size of the

719   blue circle denotes the number of ambient monitoring sites of cities.

720

721   Figure 2 Comparison of measured (black dots) and predicted (blue line) diurnal profiles of

722   near-surface hourly (a) $PM_{2.5}$, (b) O_3, and (c) NO_2 averaged over all ambient

723   monitoring stations in Beijing from 5 to 14 July 2015.

724

725   Figure 3 Comparison of measured (black dots) and simulated (black line) diurnal profiles of

726   submicron aerosol species of (a) POA, (b) SOA, (c) sulfate, (d) nitrate, and (e)

727   ammonium at NCNST site in Beijing from 5 to 14 July 2015.

728

729   Figure 4 Comparison of measured (black dots) and predicted (blue line) diurnal profiles of

730   near-surface hourly (a) $PM_{2.5}$, (b) O_3, and (c) NO_2 averaged over all ambient

731   monitoring stations in BTH from 5 to 14 July 2015.

732

733   Figure 5 Pattern comparison of simulated vs. observed near-surface $PM_{2.5}$ at 10:00 BJT

734   during the selected periods from 5 to 14 July 2015. Colored circles: $PM_{2.5}$

735   observations; color contour: $PM_{2.5}$ simulations; black arrows: simulated surface

736   winds.

737

738   Figure 6 $PM_{2.5}$ pattern variations in Beijing and surrounding areas from 20:00 BJT on July 7

739   2015 to 18:00 BJT on July 8 2015. Colored circles: $PM_{2.5}$ observations; color

740   contour: $PM_{2.5}$ simulations; black arrows: simulated surface winds.

741

742   Figure 7 $PM_{2.5}$ pattern variations in Beijing and surrounding areas from 20:00 BJT on July 10

743   2015 to 18:00 BJT on July 11 2015. Colored circles: $PM_{2.5}$ observations; color

744   contour: $PM_{2.5}$ simulations; black arrows: simulated surface winds.

745

746   Figure 8 Same as Figure 5, but for O_3 at 15:00 BJT.

747

748   Figure 9 Same as Figure 5, but for NO_2 at 08:00 BJT.

749

750   Figure 10 Temporal variations of the average contributions to the near-surface O_3 and $PM_{2.5}$

751   concentrations from total emissions (black line, defined as f_{BS}), emissions from

752   Beijing (blue line, defined as f_B), and emissions outside of Beijing (red line,

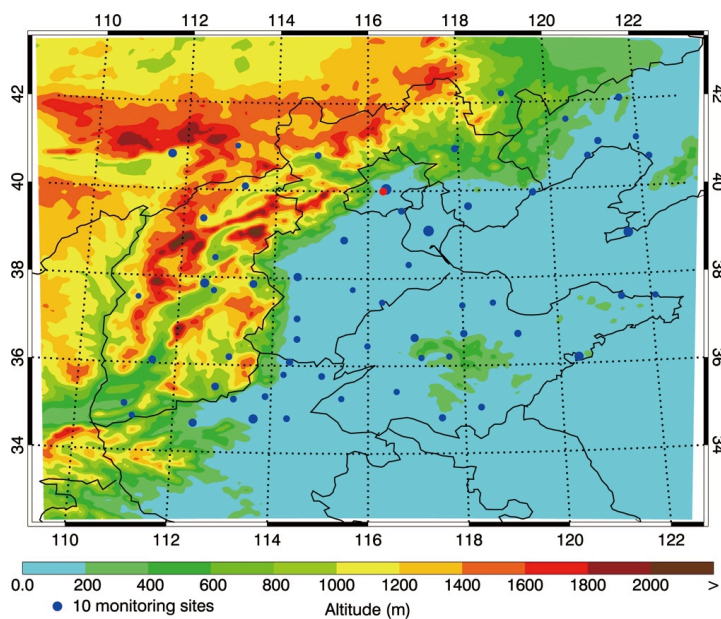753   defined as f_S) in Beijing from 5 to 14 July 2015.

754

755   Figure 11 Temporal variations of the average contributions to the near-surface aerosol

756   species concentrations from total emissions (black line, defined as f_{BS}), pure

757   emissions from Beijing (blue line, f'_B, defined as $f_B - f_0$), pure emissions

758   outside of Beijing (red line, f'_S, defined as $f_S - f_0$), the emission interactions

Atmospheric
Chemistry
and Physics
Discussions

759 (green line, f'_{BS}, defined as $f_{BS} - f_B - f_S + f_0$), and background (black dashed

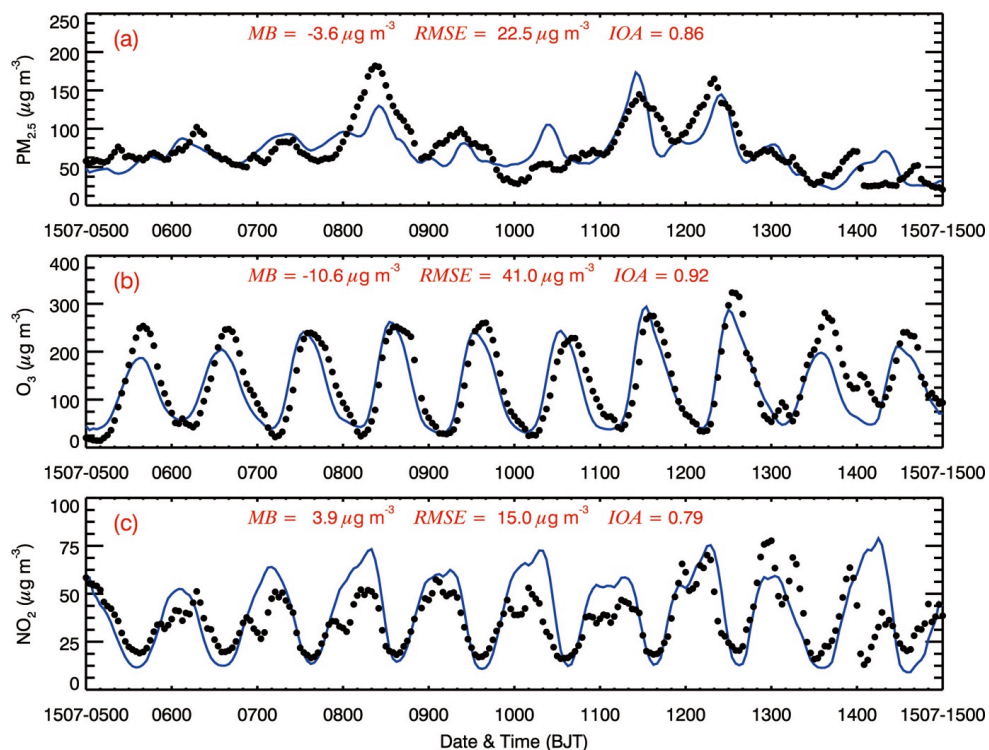760 line, defined as f_0) in Beijing from 5 to 14 July 2015.

761

762

763

764

Atmospheric
Chemistry
and Physics
Discussions

765

766
767

768   Figure 1

769
770
771
772

773

774

775   Figure 2

776

777

778

779

780
781
782   Figure 3
783
784
785
786

Atmospheric
Chemistry
and Physics
Discussions

Open Access

EGU
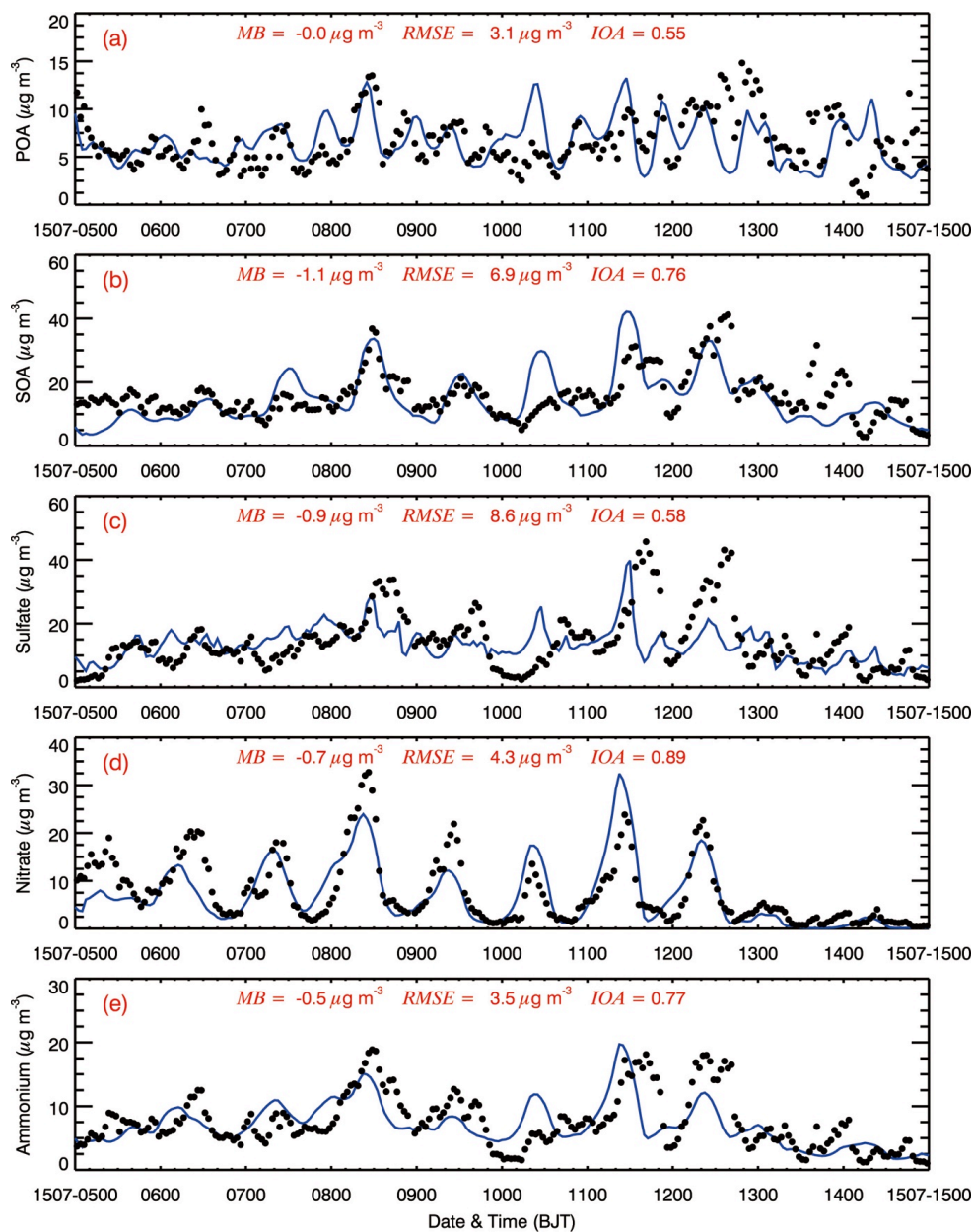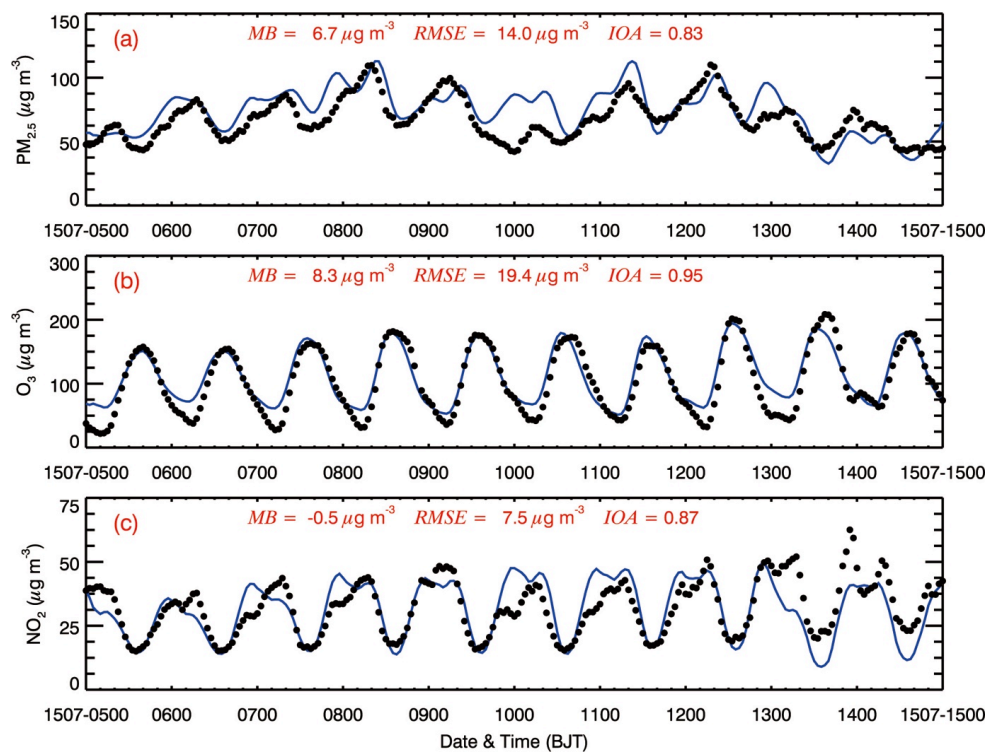
787

788

789   Figure 4

790

791

792

793

794

795

796   Figure 5

797

798

799

800

801

802

803   Figure 6

804

805

806

807

Atmospheric
Chemistry
and Physics
Discussions

Open Access

EGU
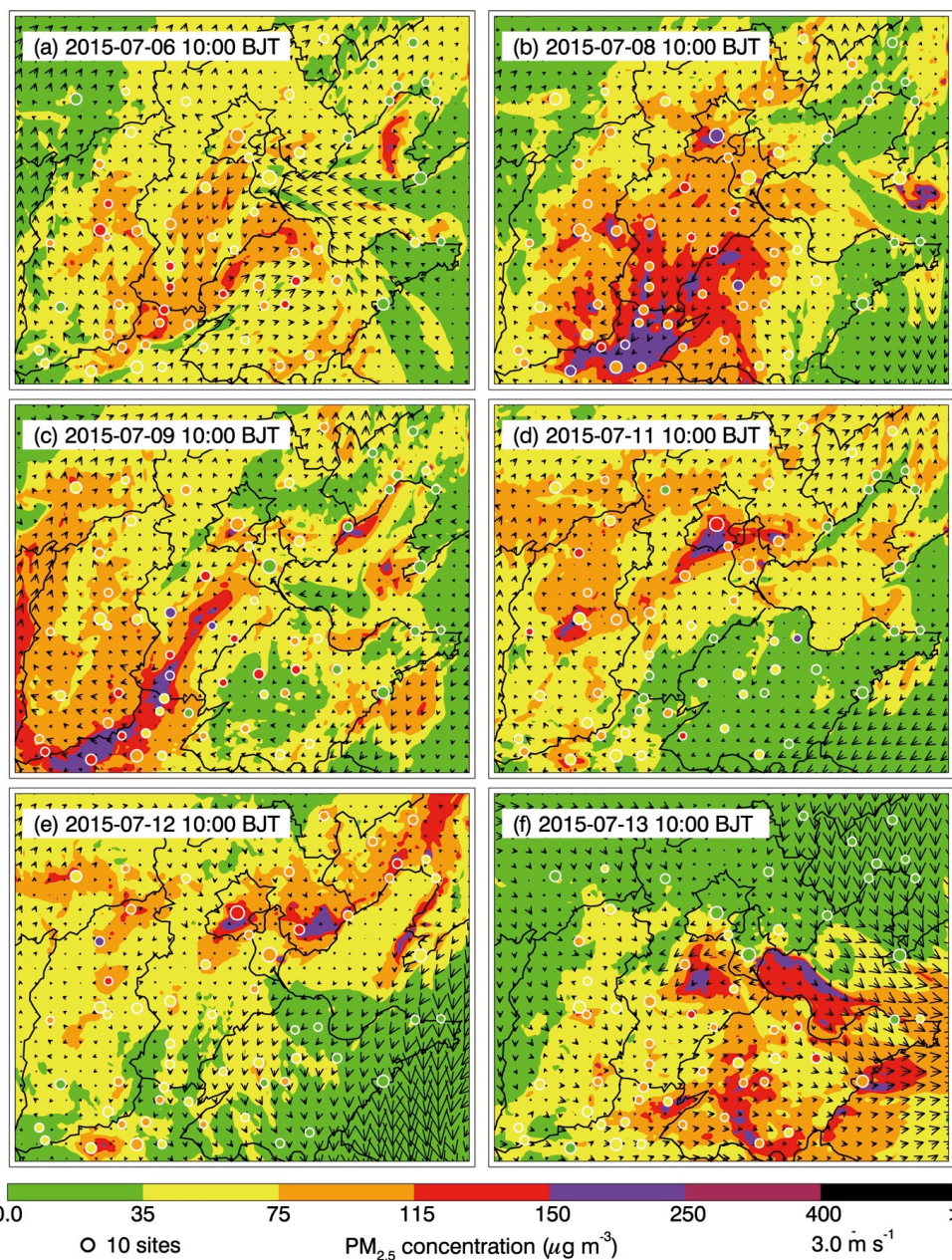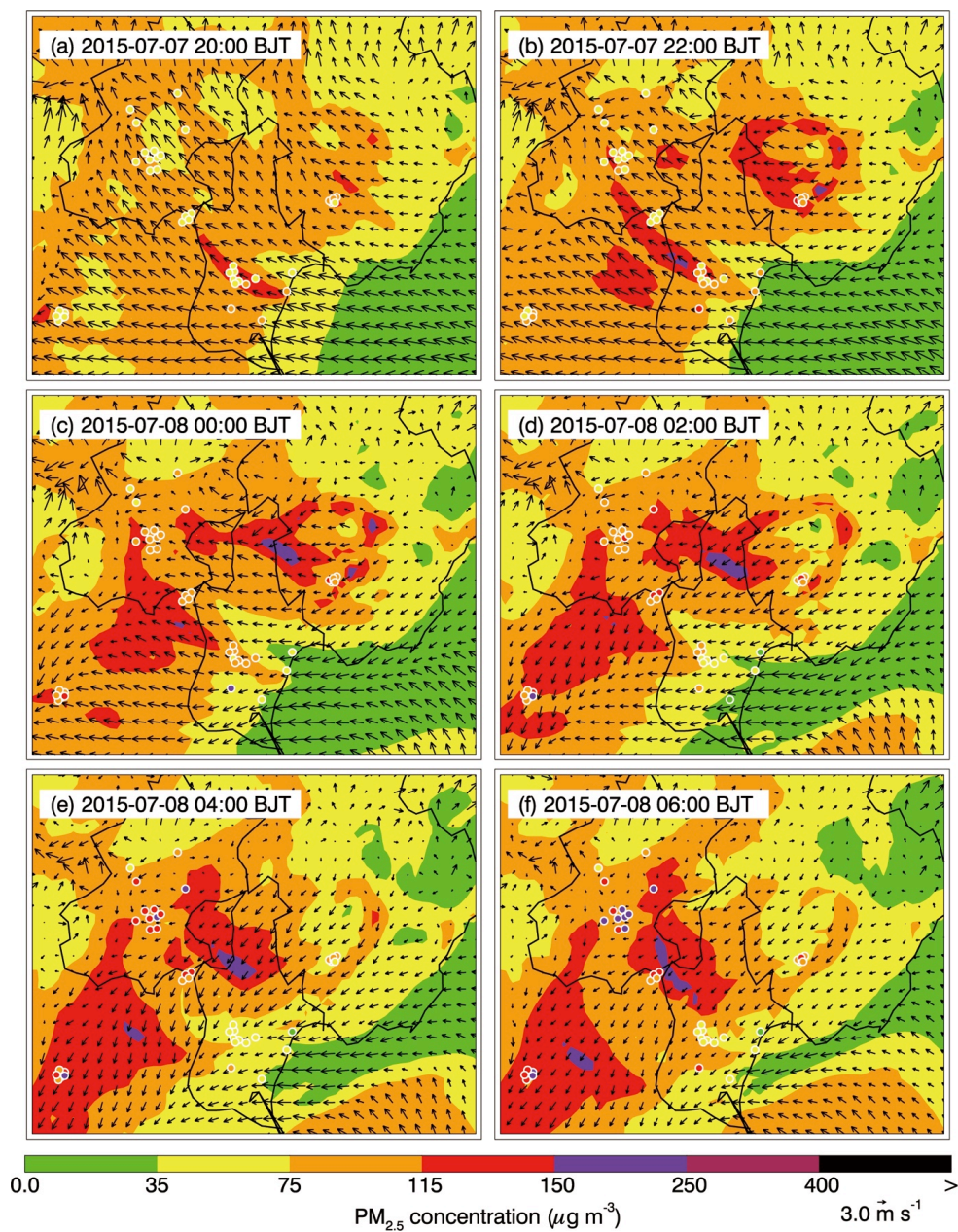
808
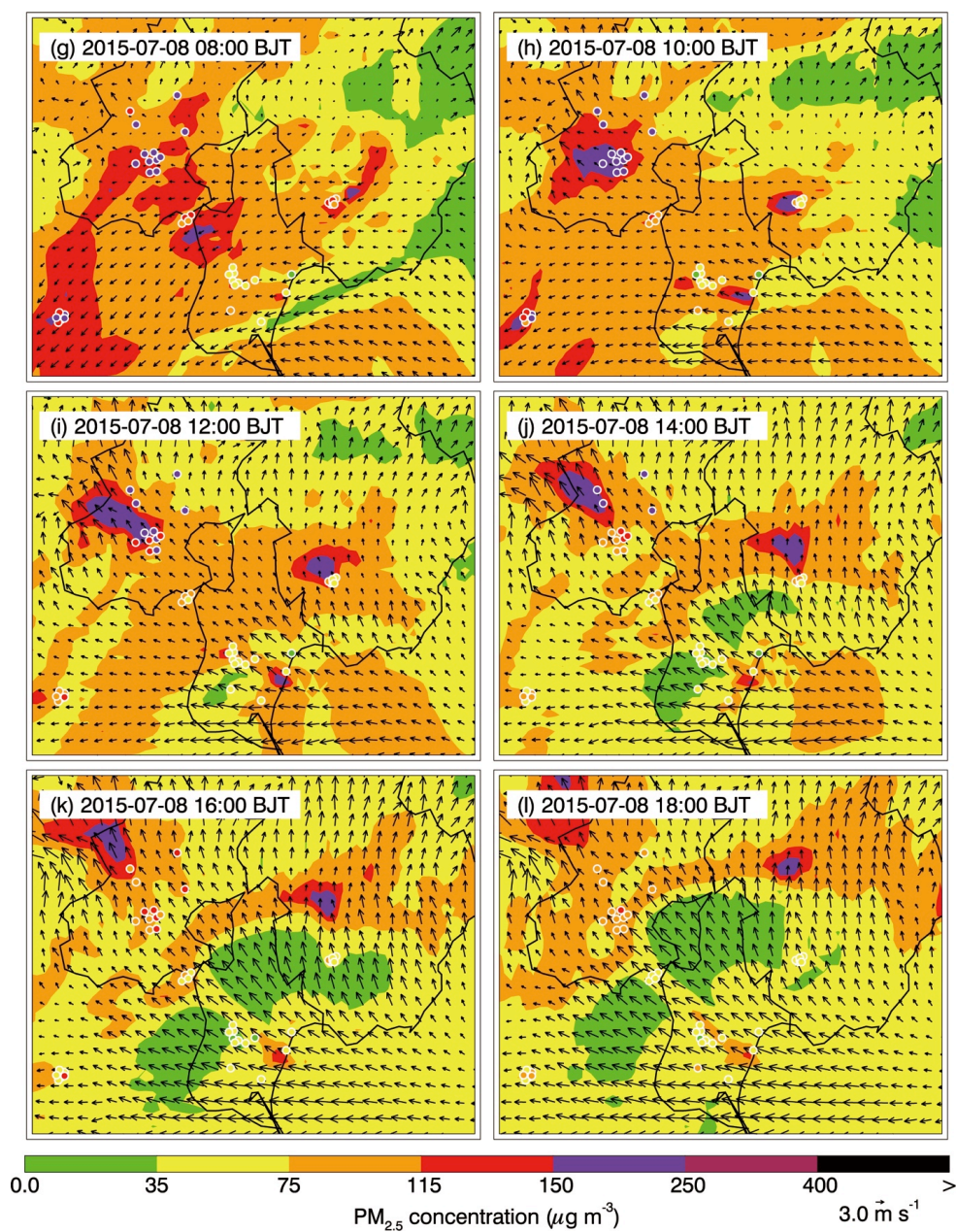
809   Figure 6 Continued
810
811
812
813

Atmospheric
Chemistry
and Physics
Discussions
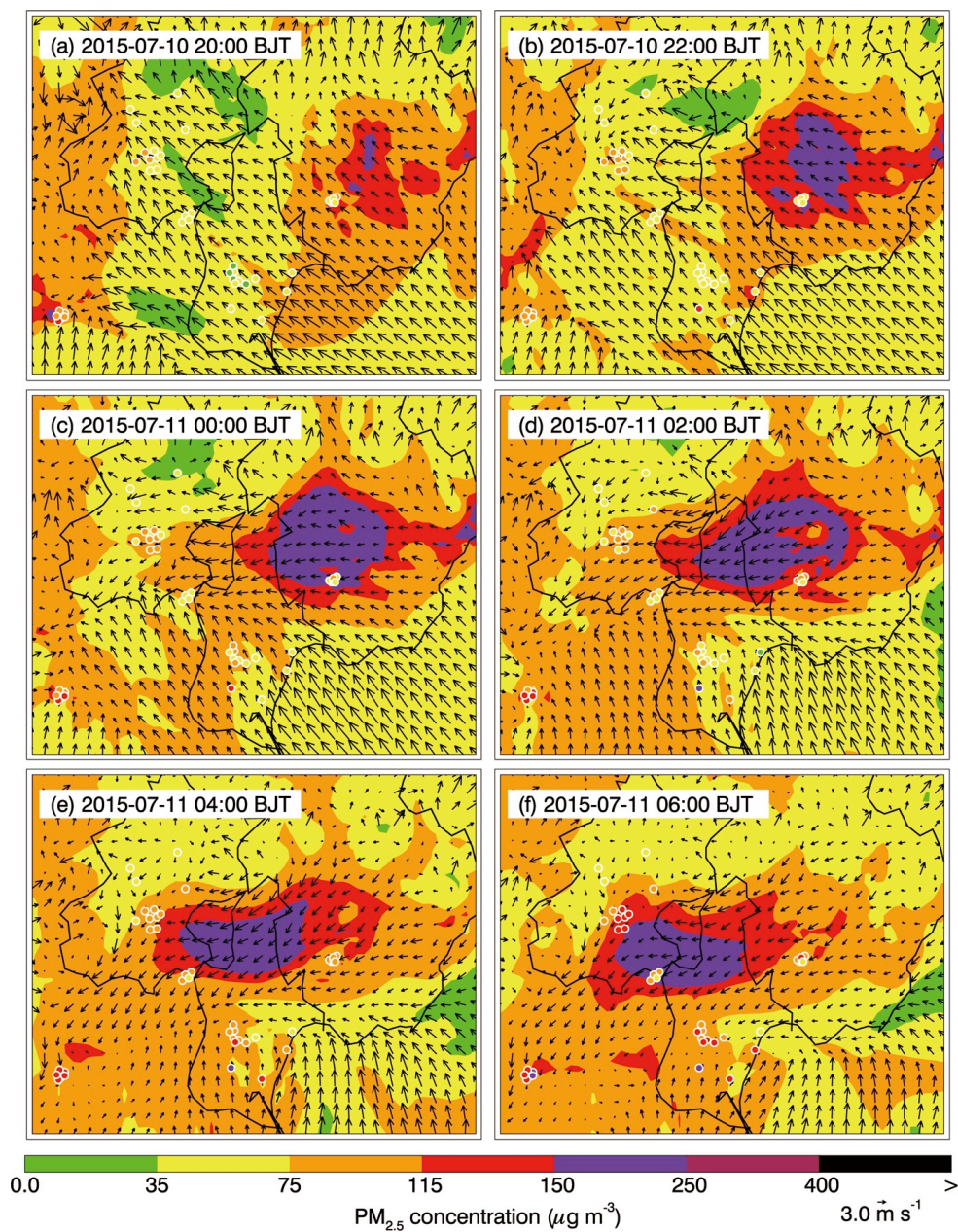
Figure 7

821
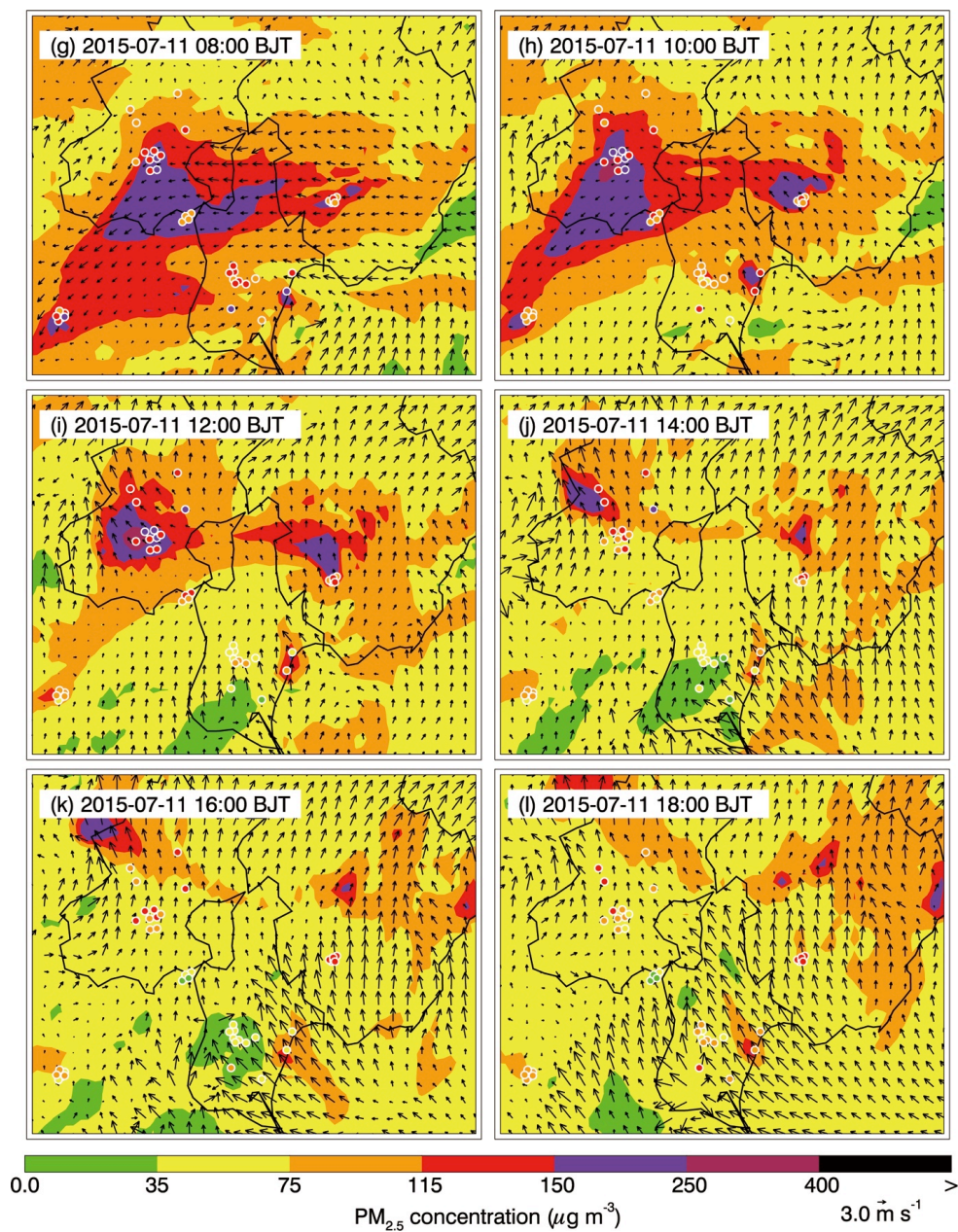
822   Figure 7 Continued
823
824
825
826

Atmospheric
Chemistry
and Physics
Discussions

Open Access

827 O 10 sites   O₃ concentration (μg m⁻³)   3.0 m s⁻¹
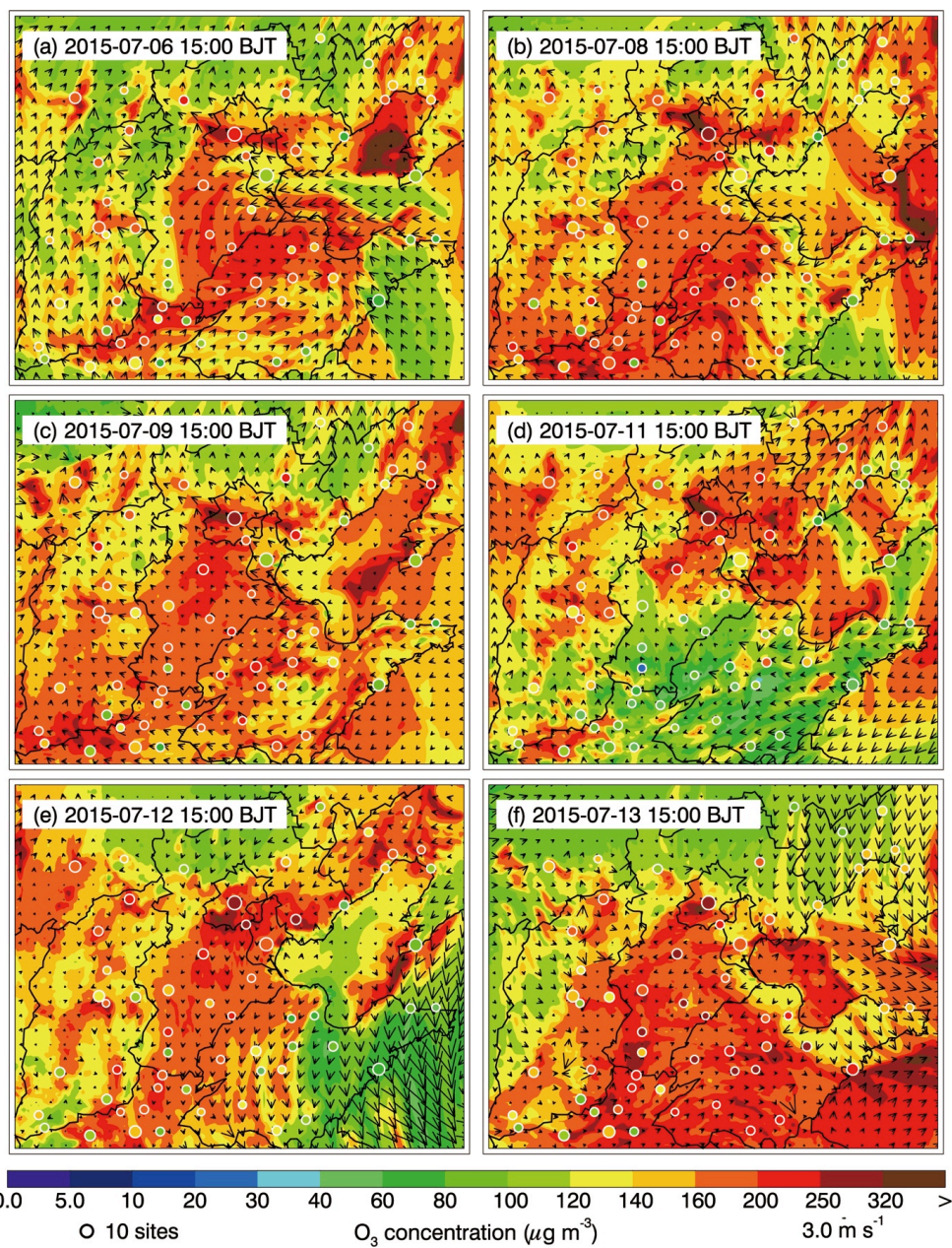
828

829 Figure 8

830

831

832

833

Figure 9

Atmospheric
Chemistry
and Physics
Discussions

Open Access
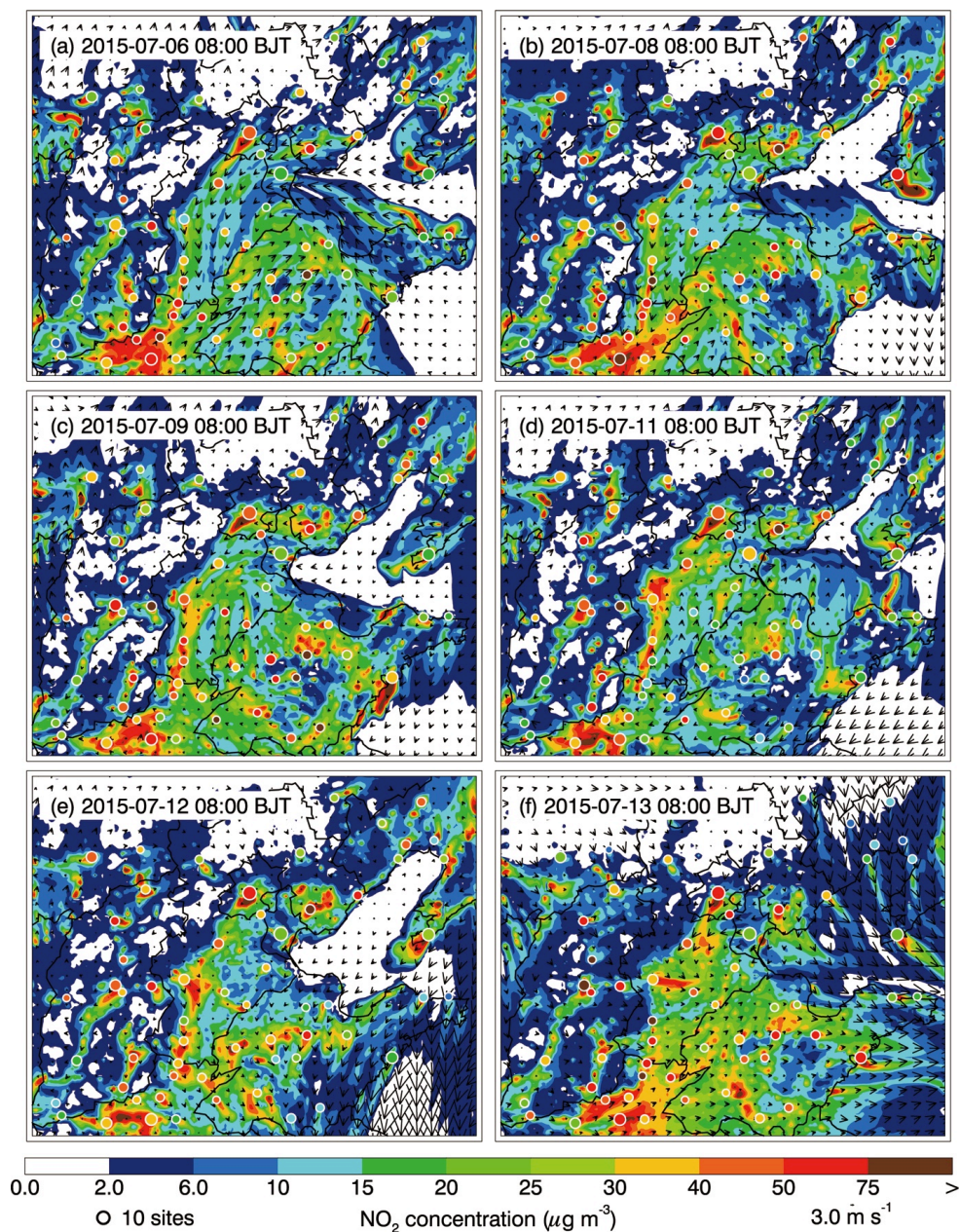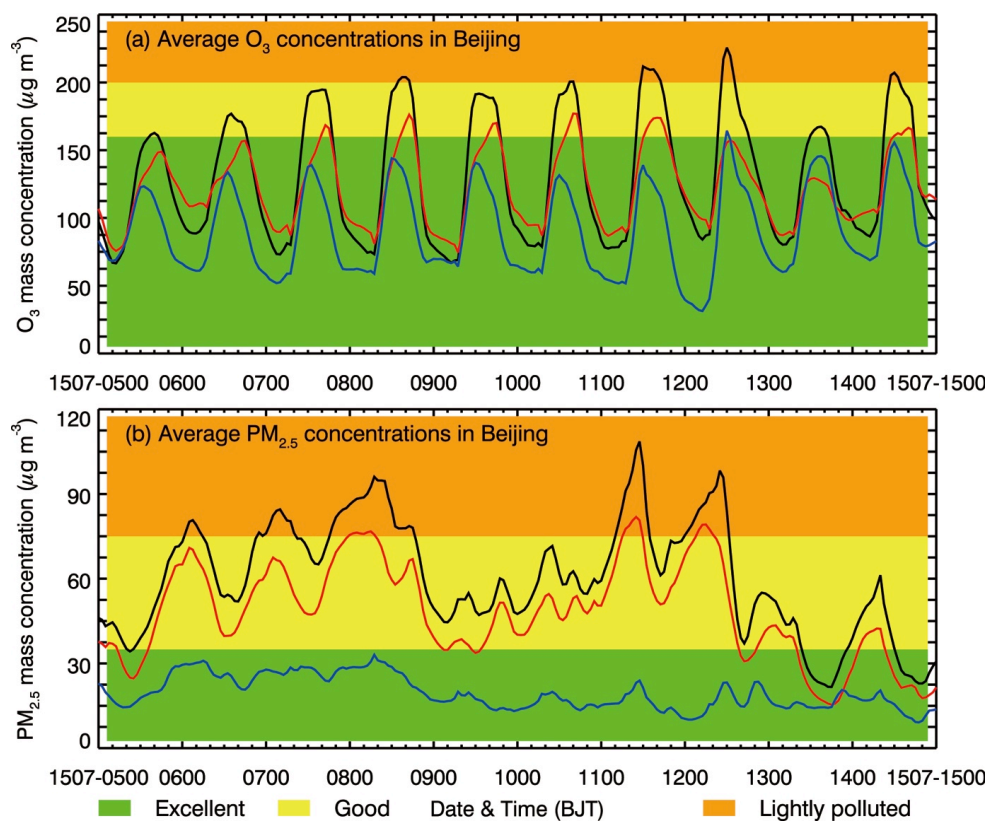
841

842

843   Figure 10

844

845

846

847

Atmospheric
Chemistry
and Physics
Discussions

Open Access
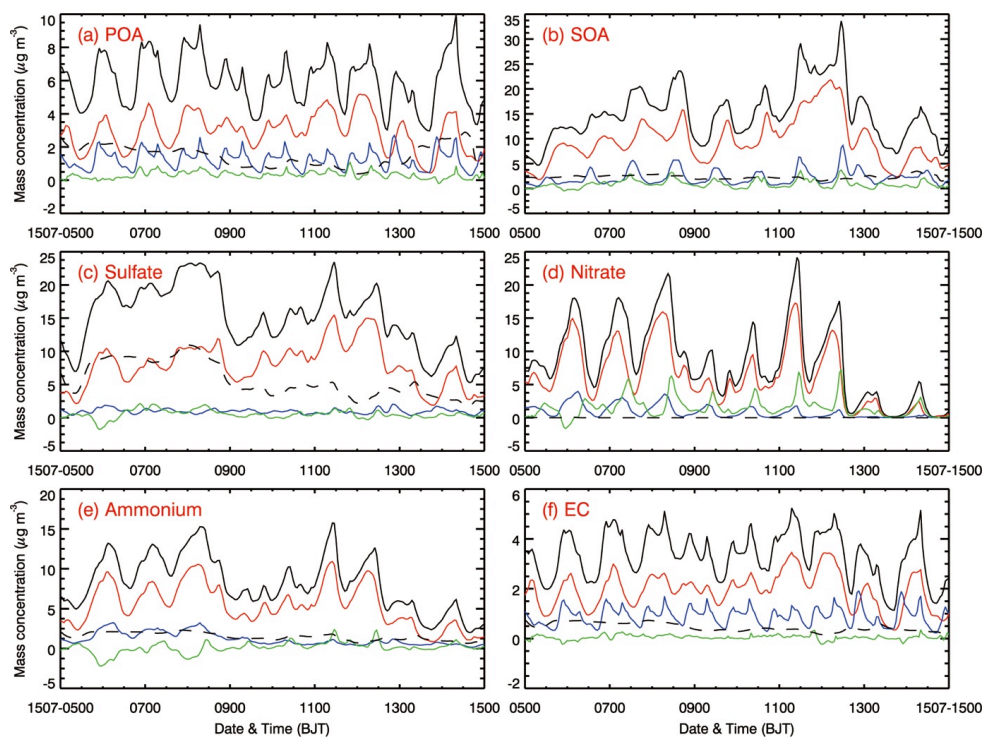
848

849

850   Figure 11

851

852

853

854